

Review

# Silica-Related Catalysts for CO<sub>2</sub> Transformation into Methanol and Dimethyl Ether

Isabel Barroso-Martín <sup>1</sup>, Antonia Infantes-Molina <sup>1</sup>, Fatemeh Jafarian Fini <sup>2</sup>,  
Daniel Ballesteros-Plata <sup>1,\*</sup>, Enrique Rodríguez-Castellón <sup>1</sup> and Elisa Moretti <sup>3</sup>

<sup>1</sup> Departamento de Química Inorgánica, Cristalografía y Mineralogía (Unidad Asociada al ICP-CSIC), Facultad de Ciencias, Universidad de Málaga, Campus de Teatinos, 29071 Málaga, Spain; isabel.barroso@uma.es (I.B.-M.); ainfantes@uma.es (A.I.-M.); castellon@uma.es (E.R.-C.)

<sup>2</sup> Department of Chemical Engineering, Isfahan University of Technology, Isfahan 8415683111, Iran; f.jafarian69@gmail.com

<sup>3</sup> Department of Molecular Sciences and Nanosystems, Ca' Foscari University of Venice, Via Torino 155, 30172 Venezia Mestre, Italy; elisam@unive.it

\* Correspondence: daniel.ballesteros@uma.es

Received: 19 October 2020; Accepted: 2 November 2020; Published: 4 November 2020



**Abstract:** The climate situation that the planet is experiencing, mainly due to the emission of greenhouse gases, poses great challenges to mitigate it. Since CO<sub>2</sub> is the most abundant greenhouse gas, it is essential to reduce its emissions or, failing that, to use it to obtain chemicals of industrial interest. In recent years, much research have focused on the use of CO<sub>2</sub> to obtain methanol, which is a raw material for the synthesis of several important chemicals, and dimethyl ether, which is advertised as the cleanest and highest efficiency diesel substitute fuel. Given that the bibliography on these catalytic reactions is already beginning to be extensive, and due to the great variety of catalysts studied by the different research groups, this review aims to expose the most important catalytic characteristics to take into account in the design of silica-based catalysts for the conversion of carbon dioxide to methanol and dimethyl ether.

**Keywords:** CO<sub>2</sub>; methanol; dimethyl ether; silica; clay; zeolites; cooper

## 1. Introduction

Deglaciation, global warming, increasingly frequent and devastating meteorological phenomena (hurricanes, typhoons, torrential rains, earthquakes, etc.) are directly related to the climate change that the planet is suffering, mainly as a consequence of emissions of greenhouse gases to the atmosphere [1]. Among these gases, it is estimated that CO<sub>2</sub> causes around 70% of global warming [2], thus being the main greenhouse gas. CO<sub>2</sub> is a product of the combustion of hydrocarbons, coal and biomass, and has long been considered a waste molecule. In combustion processes, large amounts of CO<sub>2</sub> are generated, which are emitted into the atmosphere, reaching values of 35.9 Gt of CO<sub>2</sub> per year [3] and causing the concentration of CO<sub>2</sub> in the atmosphere to have increased from 280 ppm, before the industrial revolution, up to values above 400 ppm in January 2020 [4]. The Intergovernmental Agency for Climate Change (IPCC) has warned that, if the current trend in emissions continues, the planet's average global temperature is expected to increase between 1.8 and 4.0 °C by the end of the century [5]. Therefore, it is necessary to drastically reduce CO<sub>2</sub> emissions into the atmosphere to avoid further environmental damage that could be irreversible in a short period of time, as agreed at the United Nations Climate Change Conference held in Paris in 2015, where the need to reduce greenhouse gas emissions by at least 50% in 2050 was emphasized [6].

Although most governments are taking actions to reduce the environmental impact of CO<sub>2</sub>, such as promoting the use of renewable sources, energy efficiency programs, or the implementation of palliative

strategies in various facilities, such as thermal power plants or industrial facilities, that minimize massive CO<sub>2</sub> emissions to the atmosphere, there is a long way to go for renewable energies to replace fossil fuels, thus, it is necessary to approach the issue of greenhouse gases from another point of view. There are three ways to reduce CO<sub>2</sub> production: reduce the amount of CO<sub>2</sub> produced, store CO<sub>2</sub> and use the CO<sub>2</sub> produced [7]. The first option does not seem very realistic since the global energy model is dominated by energy derived from fossil resources. Nonetheless, in recent years, CO<sub>2</sub> storage and capture technologies have been developed that are capable of capturing at least part of the carbon dioxide emitted into the atmosphere. However, in this regard, some problems arise that are currently difficult to solve, such as the long-term stability of underground storage [8,9]. Therefore, from the scientific community, CO<sub>2</sub> has gone from being a waste molecule to an important resource/raw material, which is why the CO<sub>2</sub> molecule has begun to be considered as a resource to produce products and fuels with high added value.

Considering CO<sub>2</sub> as a raw material also has certain advantages, such as that, being a waste material, its cost as a raw material is zero. In addition, recycling and/or using CO<sub>2</sub> directly at the production sites avoids additional costs derived from transport, which can represent up to 35–40% of the total cost of the CO<sub>2</sub> capture and storage processes [10]. Last but not least, another important advantage is that CO<sub>2</sub> recycling/use is socio-politically accepted. Currently, CO<sub>2</sub> used as a chemical feedstock in the industry only represents about 1/3 of the annual atmospheric emissions [3]. Therefore, it is necessary to develop new economic processes that utilize CO<sub>2</sub> to reduce emissions [11]. The scientific community has proposed a wide range of possibilities to use CO<sub>2</sub> to produce high-value-added products through catalytic processes, such as dry reforming of methane [12], copolymerization reactions [13], oxidative dehydrogenation (ODH) of light alkanes [14], methanation [15], oxidative coupling of methane [16] or hydrogenation of carbon dioxide, among others, so that a CO<sub>2</sub> closed cycle can be established, where “spent carbon” such as CO<sub>2</sub> is converted into “working carbon” that is present in valuable chemicals or fuels. However, the CO<sub>2</sub> molecule has a high oxidation state and is also very thermodynamically stable ( $\Delta G_f = -396 \text{ kJ}\cdot\text{mol}^{-1}$ ), it must be combined with high-energy reagents, together with effective catalysts and at the conditions of thermodynamically favorable reaction [1] to obtain high value-added or combustible products. Therefore, the development of processes and/or products that are less harmful to the environment and mainly focused on reducing global warming is one of the main challenges facing the scientific community.

Among the conversion of CO<sub>2</sub> into chemicals, the synthesis of dimethyl carbonate [17], urea [18] and light olefins [19] should be highlighted. Besides, there is another option in which CO<sub>2</sub> is transformed into reduced forms, that is, oxidation states 2, −2 and −4, leading to the formation of CO and hydrogenated products such as methanol (MeOH), dimethyl ether (DME), methane, hydrocarbons, etc. [20–23], through several reactions, being one of the most studied forms of CO<sub>2</sub> hydrogenation, which is regarded as the most effective way to approach the environmentally friendly synthesis of sustainable chemicals and fuels [24–27], which have much greater relevance.

#### *CO<sub>2</sub> Hydrogenation to Methanol and Dimethyl Ether*

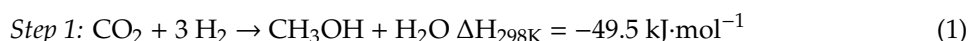
Annual global methanol production in 2018 was 79 million metric tons [28]. Today, methanol is produced almost exclusively from syngas and is of great importance in the chemical industry, as it is a raw material for the synthesis of several important chemicals such as chloromethane, acetic acid, methyl tert-butyl ether, alkyl halides, formaldehyde and dimethyl ether. The latter can be used in fuel cells and diesel engines [29,30]. Hydrogenation of CO<sub>2</sub> to MeOH (Equation (1)) is thermodynamically favorable but requires the use of catalysts to overcome the high-activation energy barrier. However, it leads to the formation of other by-products during the hydrogenation of CO<sub>2</sub>, such as CO, hydrocarbons and even higher alcohols. For this reason, highly selective heterogeneous catalysts are necessary to enhance methanol production by CO<sub>2</sub> hydrogenation.

Thermodynamically, both a decrease in the reaction temperature and an increase in the reaction pressure can favor the synthesis of methanol (MeOH) [23,31,32]. At temperatures higher than 240 °C,

the activation of CO<sub>2</sub> and, consequently, the formation of methanol, is facilitated [22]. However, it has been observed that high temperatures also lead to a low MeOH production, as side reactions towards hydrocarbons and higher alcohols can take place.

Along with the production of methanol, the production of dimethyl ether (DME) from CO<sub>2</sub> has attracted great interest. DME can be produced from different sources such as biomass, coal and natural gas. It is generally produced directly from syngas with a small amount of CO<sub>2</sub> or by dehydration of methanol derived from syngas. The separation of products (DME, water, methanol) is carried out via distillation and leads to products with high purity [33]. In 2010, 6.7 Mt of DME was produced worldwide, of which 8% came from this process [34,35]. The influence and demand of DME, obtained from sustainable sources, will continuously increase in the coming decades: approximately 5 million metric tons were produced in 2016 and global production is expected to exceed 20 million metric tons in 2020 [36]. Therefore, the development of efficient processes and catalysts are the basic requirements to satisfy this growing demand [35]. The use of DME as fuel has several advantages, among others: DME is neither toxic nor carcinogenic [37]. Its physical–chemical properties are close to liquefied petroleum gas (LPG), which allows the technologies employed in LPG to be easily adapted for DME [38]. Apart from its use as a fuel, DME is also used to obtain other products of great industrial interest, such as dimethyl sulfate, methyl acetate and light olefins [39]. During the combustion of DME, low emissions of particles, CO and NO<sub>x</sub> are generated whereas SO<sub>x</sub> is not produced, and the lack of C–C bonds in DME molecules limits the formation of carbon soot during the combustion of the fuel, which is a typical problem for diesel engines [40,41]. DME has a high cetane number, higher than diesel fuel (ULSD is 40–55) [41,42], which, together with its low boiling point (−25 °C), make it have a lower ignition delay and improves the fuel–air mixture, reducing cold start problems.

However, using DME as fuel has some drawbacks that need to be addressed before it can replace fossil fuels. DME has low lubricity and high volatility, so its direct use in current engines is not feasible, so it is necessary to adapt current engines to DME [41,43]. Another disadvantage of DME is that it has half the energy density of diesel, so it is necessary to use fuel tanks twice as large as diesel. The synthesis of DME from CO<sub>2</sub> can be carried out in two stages, as mentioned above, first forming methanol with a metal catalyst (Equation (1)) and followed by dehydration with an acid catalyst (Equation (2)).



It is also possible to synthesize DME in a single stage, using a bifunctional catalyst that produces methanol and causes its dehydration in the same reactor (Equation (3)) [44]. As in the case of MeOH, the one-step reaction is thermodynamically favorable (Equation (3)).



The one-step process is more interesting since it reduces investment and operating costs, as only one reactor is required [45,46], and it is possible to eliminate the accumulation of methanol in the reactor, which generally avoids the CO<sub>2</sub> conversion to reach thermodynamic equilibrium. In any case, the need to use an efficient catalyst to obtain a high production of MeOH and DME is essential. Currently, bifunctional catalysts for the synthesis of DME have been oriented to copper-based catalysts or noble metal catalysts as the hydrogenation component, and solid acid catalysts such as HZSM-5, HZSM-22, SAPO-34, SAPO-57, SAPO-59 and HSSZ-13 for the dehydration component [47,48]. Copper-based catalysts have been widely used for the CO<sub>2</sub> to methanol hydrogenation process because they can operate at relatively high temperatures and pressures [49]. Given the studies that have been carried out in recent years on the production of methanol and dimethyl ether from the hydrogenation of carbon dioxide, this review tries to bring together the main studies on the use of silica-based catalytic supports (although they are not very abundant), due to its good properties and low cost.

## 2. Two-Step Synthesis of DME

In the CO<sub>2</sub> hydrogenation reaction to obtain MeOH (Equation (1)), there are two key factors in designing a good catalyst. On the one hand, the high temperatures required to obtain a good yield towards MeOH lead to sintering and agglomeration of the active phase [50] and, on the other hand, one of the three hydrogen molecules necessary for the hydrogenation of CO<sub>2</sub> is consumed in the formation of water, which is a strong oxidant, resulting in the oxidation of the metallic phases present in the catalyst [51]. The same occurs in the second step (Equation (2)) of dehydration of MeOH to obtain DME. In any case, the deactivation of the catalyst usually occurs.

A wide variety of active phases in the CO<sub>2</sub> hydrogenation reaction to obtain MeOH and DME has been studied, mainly based on transition metals for their ability to accept or donate electrons. However, the support used in the catalyst formulation is also of paramount importance for the proper functioning of the catalyst. In heterogeneous catalysis, the main objective of the support is to improve the dispersion of the active phase. One of the most studied supports in the CO<sub>2</sub> reaction to obtain MeOH and DME is silica (SiO<sub>2</sub>), either in the form of pure silica or silicon atoms forming part of zeolites or clays. Among others, mesoporous silicas have been widely studied due to their high dispersion capacity, thermal stability and high superficial area. Regarding the active phase, copper is one of the most used metals for this reaction and, although it is highly active, its catalytic capacity is notably improved with the help of promoters. When working with copper, the Cu<sup>+</sup>/Cu<sup>2+</sup> ratio is one of the determining factors in the proper functioning of this catalyst; the higher the Cu<sup>+</sup>/Cu<sup>2+</sup> ratio, the better the catalytic performance due to the formation of Cu<sup>+</sup> species, so that there are redox pair sites available. Instead, the presence of Cu<sup>2+</sup> species is detrimental to the formation of MeOH and DME [52–54]. Regardless of the catalyst configuration, whether or not metal phases are used, the strength of the acid–base pairs and their nature (Lewis or Brønsted) is one of the most determining factors for its appropriate functioning. Although a relationship between the rate of dehydration of methanol and the number of Brønsted acid sites has not yet been established [55], it is well known that the stronger the Brønsted acid sites, the lower the reaction temperature required to achieve a good catalytic performance. However, Brønsted acid sites have been reported to promote DME reactions to form olefins if they are strong enough, as suggested by A.M. Bahmanpour et al. [55], while Lewis acid sites tend to favor the dehydration of methanol to DME but not to hydrocarbons [55–57]. If the Brønsted acid sites are not strong enough, the formation of olefins does not occur and less carbon deposits are observed on the surface, improving the catalyst stability. Therefore, Brønsted/Lewis ratio, as well as its strength, is a determining factor in the MeOH conversion and the selectivity to DME [55,58–61].

### 2.1. Catalysts Based on Pure or Doped Silica

Mesoporous silicate structures (MCM family, SBA, etc.) have been widely employed as a support or promoter component of a heterogeneous catalyst for CO<sub>2</sub> hydrogenation. MCM and SBA materials are mesostructured silicas that were discovered in the early 1990s by the Mobil 1–3 Corporation and that have been widely used in heterogeneous catalysis and as adsorbents because their properties, such as their high surface area (>600 m<sup>2</sup>/g) and narrow pore size distribution, in the range of mesopores (2–50 nm), according to the IUPAC classification [62], what facilitates mass transfer through pores. Likewise, to selectively produce DME, optimal acidity is required, which can be achieved either by incorporating metal ions into the structure or by changing the preparation process, although the presence of strong acid sites causes side reactions and coke formation which decreases the useful life of a catalyst [63–65]. Several researchers have tried to increase the acidity of MCM-41 type silica. Therefore, a composite molecular sieve like the one studied by Tang et al. [66], consisting of MCM-41 and ZSM-5, has shown remarkable catalytic activity and selectivity to DME in the methanol dehydration (see Table 1) thanks to the combination of MCM-41 mesoporosity and the ZSM-5 acidity and stability. Other research groups have attempted to improve the catalytic properties of MCM-41 SiO<sub>2</sub> by incorporating metal ions such as Fe, Ga, Al, Mn, Ni, Co, etc., [67] capable of providing the mesoporous support with the

acidity required in the dehydration of methanol to DME. Sang et al. [68] prepared MCM-41 doped with various types of metal ions (Al, Ga, Sn, Zr and Fe). Their results show that aluminum is the metal with the best performance among the cations studied. Although Sn and Zr are more acidic ions than aluminum, their higher ionic radius hinders their incorporation into the MCM-41 structure, which leads to lower catalytic performance. Much of the effort has been focused on the use of SBA-15 as a mesoporous support for CO<sub>2</sub> hydrogenation. Many studies have shown that SBA-15 perform well as a catalyst support due to its flexible pore structure and large specific surface area [69–71], as well as its hydrothermal stability. As already mentioned, the type of acidity (Lewis or Brønsted) is important to obtain a higher selectivity towards methanol or DME. Herrera et al. [72] used tungsten oxide as the active component (due to its stronger Brønsted acid sites compared to other transition metal oxides [73–75]), supported on SBA-15 for methanol dehydration. However, the preparation method and the W/Si ratio can affect its structure and catalytic performance, reporting that a small W/Si ratio leads to less Brønsted acid sites and calcination temperatures higher than 400 °C cause a decrease in the Brønsted acidity and, consequently, the selectivity towards DME [63].

**Table 1.** Silica-based catalysts for MeOH dehydration to DME.

Catalyst	T (°C)	P (Bar)	MeOH Conversion (%)	DME Selectivity (%)	Ref.
ZSM-5/MCM-41 (SiO <sub>2</sub> /Al <sub>2</sub> O <sub>3</sub> = 20)	210	1	86.7	100	[66]
Al/MCM-41 (SiO <sub>2</sub> /Al <sub>2</sub> O <sub>3</sub> = 10)	300	1	50	100	[68]
STA <sup>a</sup> /SiO <sub>2</sub> (W/Si = 0.33)	250	1	60	99	[63]
Al-MCM-41 (SiO <sub>2</sub> /Al <sub>2</sub> O <sub>3</sub> = 30)	260	50	73	97	[64]

<sup>a</sup> Silicotungstic acid.

Cu-based catalysts have been extensively used for the carbon dioxide hydrogenation to methanol. Their catalytic activity has been related to large copper surface area, high dispersion and good interaction between copper and the oxide support [76–78]. Tasfy et al. [79] prepared a series of Cu/ZnO supported on SBA-15 with different metal loadings and observed that higher metal loadings favor the formation of agglomerates that worsen the catalytic activity and methanol selectivity due to the improvement in the water gas shift reaction rate, forming more CO and water. In another study, Min et al. [80] investigated the addition of Zr and Mn on Cu-ZnO/SBA-15 samples in the catalytic performance of the CO<sub>2</sub> hydrogenation to methanol. The presence of oxides improved the catalytic performance by increasing the copper dispersion, leading to an easier reduction in CuO species. Moreover, Zr additive showed better methanol selectivity and yield by increasing the catalyst acidity and the oxygen vacancies concentration. Based on these results, Koh et al. [67] used different transition metal oxides (Cr, Mn, Fe, Co, Ni) to promote the catalytic performance of Cu-ZnO/SBA-15 in the same reaction. Their results showed that not only the copper crystallites size but also the degree of interactions between copper oxide and other oxide species in the catalyst can affect the catalytic performance. Table 1 summarizes some of the silica-based catalysts that have been used in the synthesis of methanol and dimethyl ether from the hydrogenation of CO<sub>2</sub>.

## 2.2. Clay-Based Catalysts

Clay-based materials have attracted great attention as catalysts, due to their abundance in nature, low cost, and environmentally friendly properties [81–84]. Furthermore, they show a unique combination of characteristics such as high ion exchange capacity, porosity, Lewis and Brønsted acidity and a wide variety of compositions, textures and layered structures, which make these aluminosilicates very interesting to apply in a variety of catalytic reactions. The main advantage of clays is that their structural, textural and acidic properties can be modified by incorporating cations or metallic oxides in their structure. However, clay intercalation methods have a relatively high cost and also lead to irreproducibility issues, which could explain the scarce research focused on these materials to obtain MeOH and DME from CO<sub>2</sub> hydrogenation. Despite this fact, it is possible to treat the clay directly

without incorporating other metallic phases, taking advantage of the fact the deposited minerals naturally contain many cations such as Si, Al, Fe, Mg or Ca, for example, subjecting it to thermal and/or acid treatments that modify its acidity, structural and textural properties, and is also a way to reduce costs [85–88]. Montmorillonite has been one of the most investigated clay materials as a catalyst for the dehydrogenation reaction of methanol to dimethyl ether. This clay, which belongs to the smectites group, has relevant intercalation properties and can be inserted relatively easily between its metallic oxide sheets that form pillars so that it is possible to control the pore structure and, with it, the catalytic properties of the system. One of the most used montmorillonite modifications is the insertion of aluminum cations in its lamellar structure, since it provides acidity (Lewis and Brønsted sites of strong nature) and thermal stability, and it also increases the specific surface area [89]. Although alumina by itself does not offer the best catalytic results in this reaction, the increase in surface area and porosity that alumina provides gives an opportunity to introduce other more catalytically active metal phases. According to L. Chmielarz et al. [90], the deposition of aluminum with tetrahedral coordination takes place mainly on the surface, minimizing the loss of porosity, increasing pore size and avoiding pore blockage caused by the intercalation of montmorillonite and, in addition, the surface concentration of acid sites increases significantly with the formation of stronger acid sites, mainly Lewis-type. The same conclusions can be drawn from the study carried out by W. Pranee et al. [88], where they argue that  $\text{Al}^{4+}$  are associated with increased methanol conversion because they do not induce water molecules' formation, allowing methanol molecules to be closer each other. The formation of water blocks methanol formation and inhibits its adsorption on the active sites because water competes with methanol for Lewis acid sites [59], and this occurs when there is a higher concentration of  $\text{Al}^{5+}$  and  $\text{Al}^{6+}$ .

The incorporation of Nb [91], Ti or Zr [59,92] in clay-based catalysts substantially reduces the amount of Lewis acid sites and, in the case of Ti and Zr, giving rise to Brønsted acidity, that does not favor MeOH dehydration to DME.

As mentioned above, copper is by far the most studied and applied metal in this reaction. F.C.F. Marcos et al. [91] prepared Cu-Nb and Cu-Ce bimetallic catalysts by impregnating montmorillonite with the alumina pillars. They observed that the incorporation of Nb and specially Ce improves the  $\text{Cu}^+/\text{CuO}$  ratio, which favors higher conversions and selectivities. Table 2 summarizes some of the clay-based catalysts that have been used in the synthesis of methanol and dimethyl ether from the hydrogenation of  $\text{CO}_2$ .

### 2.3. Zeolites Based Catalysts

$\gamma\text{-Al}_2\text{O}_3$  has traditionally been used as the benchmark catalyst for the methanol dehydration thanks to its high activity and selectivity to DME [93]. However, the need for a high reaction temperature over 300 °C and its sensitivity to the presence of water, a reaction by-product, has promoted the quest for different catalysts for this reaction [94], such as  $\text{Al}_2\text{O}_3\text{-B}_2\text{O}_3$  [95], clay [55] or zeolite-based materials [96–98]. Zeolites have been one of the most studied catalysts thanks to their unique properties that allow a high activity and selectivity towards DME formation even at relatively low temperatures (below 300 °C). Zeolites are crystalline inorganic silicate-based materials that can be both natural and synthetic. Their well-defined microporous structure consists of a framework of  $\text{TO}_4$  tetrahedra, with vertex-sharing aluminate  $[\text{AlO}_4]^-$  and silicate  $\text{SiO}_4$  and cations out of the framework to balance the negative charge. These tetrahedral structures can be arranged in secondary building units that, in turn, can form cages and channels which confer them great 3-D shape selectivity and also high specific surface area [99], which are key factors in catalysis. Likewise, thanks to their composition, zeolites present both Lewis and Brønsted acidity which is essential in many catalytic processes, such as oil cracking. Although acidity in zeolites is indicative of remarkable catalytic performance, strong acid sites have been reported to promote the DME conversion to by-products such as aromatic species, lessening the yield of methanol dehydration to the DME process and promoting the coke formation, the latter being the main reason for the zeolites deactivation, since they can be adsorbed on active sites of the catalyst, provoking pore blockage. Guisnet et al. [100] explained this fact by relating the role

of the strength and density of acid sites in zeolites in the coke formation with the rate of chemical steps taking place in the reaction. The faster these steps, the more prone to the formation of heavy molecules, and the higher the density of acid sites, the greater the number of chemical steps along the diffusion path, which facilitates condensation reactions that promote coke formation. Many approaches have been studied to control the zeolites' acidity and optimize the methanol dehydration reaction, such as the modification of the Si/Al ratio [101], as seen hereafter, or metal impregnation, which has been shown to reduce strong acidity and, therefore, enhance its catalytic performance and reduce coke formation. In fact, H-ZSM-5 impregnated with Zr has been reported to show a 16% increase in methanol conversion and a 31% increase in DME selectivity thanks to the weaker acidity of the impregnated zeolite [102]. It is also well-known that the zeolites' topology, including both channel opening and channel orientation, also influences the coke formation. As a general rule, it could be said that zeolites with larger pores, such as those with BEA frameworks (three-dimensional zeolite), CHA (SAPO-34, large channel intersections with narrow openings) or AFI types (mono-dimensional, aluminophosphate AlPO-5 zeolite) with a 12-ring structure, are more susceptible to deactivation by coke than those of medium pore, such as the MFI type with a 10-ring structure (ZSM-5) [94,103,104]. Finally, the reaction temperature has been proved to strongly influence the composition of carbon deposits. At temperatures below 300 °C, coke mainly consists of light aromatic compounds, whereas at higher temperatures polycyclic compounds are formed [105]. Thus, a trade-off reaction temperature must be achieved to minimize coke formation and maximize conversion and selectivity to DME. Table 3 summarizes some of the zeolite-based catalysts that have been used in the synthesis of dehydration from methanol to dimethyl ether.

**Table 2.** Clay-based catalysts for MeOH dehydration to DME.

Catalyst	T (°C)	P (Bar)	MeOH Conversion (%)	DME Selectivity (%)	Ref.
Allophane pure	275	1	77	97	[60]
Palygorskite treated with HNO <sub>3</sub>	275	1	38	98	[60]
Sepiolite treated with HNO <sub>3</sub>	275	1	18	96	[60]
(V/S/Al) <sub>oxalic acid</sub>	450	1	30	100	[59]
(V/S/Ti) <sub>oxalic acid</sub>	450	1	3	78	[59]
Vermiculite (PILC)	250	1	18	100	[92]
PILC-Al <sup>a</sup>	250	1	55	99	[92]
(PILC-C-Al) <sup>a</sup> citric acid	250	1	70	99.5	[92]
(PILC-O-Al) <sup>a</sup> oxalic acid	250	1	50	98	[92]
PCH <sup>b</sup> -Si	250	1	77	100	[90]
PCH <sup>b</sup> -Al	250	1	85	100	[90]
PCH <sup>b</sup> -Ti	250	1	68	100	[90]
PCH <sup>b</sup> -Zr	250	1	73	100	[90]
Montmorillonite	250	1	15	-	[90]
DM <sup>c</sup> sulfuric acid	300	1	10	100	[88]
DM <sup>c</sup> hydrochloric acid	300	1	16	95	[88]
DM <sup>c</sup> nitric acid	300	1	35	80	[88]
DM <sup>c</sup>	300	1	10	98	[88]
K10-C300 <sup>d</sup>	300	1	80	100	[55]

<sup>a</sup> Al/vermiculites ratio = 10 mmol Al per 1 g of clay mineral. <sup>b</sup> PCH: Intercalation of montmorillonite with silica pillars.

<sup>c</sup> DM: diatomite. <sup>d</sup> Montmorillonite K10 calcined at 300 °C.

ZSM-5 zeolite is one of the most studied catalysts for methanol dehydration. It consists of pentasil (eight five-membered rings) units linked by oxygen bridges creating the MFI cavity. Besides, a 10-ring opening is formed, giving rise to 3-D microporous channels [104,110]. Because of its high acidity and microporous channels structure, the diffusion and removal of large molecules is difficult, and conventional ZSM-5 zeolite is quickly deactivated by coke deposition. This drawback can be overcome by modifying some of the physicochemical properties of the zeolite, such as the Si/Al ratio, porosity, crystal size or its framework by introducing an ion into it [111]. Regarding the Si/Al ratio

modification, it is usually carried out through a post-synthesis treatment. Aloise et al. [109] reported that acidity of the desilicated ZSM-5 increased by 42% after a 60 min desilication treatment, due to both new Brønsted and Lewis acid sites created thanks to the partial extraction of Al from tetrahedra to extra-framework positions. The mesoporosity was induced in the zeolite, creating a hierarchical system that facilitated accessibility to the zeolite microporous structure which, together with the increase in acidity, led to better catalytic performance while maintaining ZSM-5 high product selectivity to DME. Likewise, Catizzzone et al. [94] reported that a higher aluminium concentration in FER-type zeolites led to a higher methanol conversion at low temperatures (160–240 °C) thanks to the increase in Lewis acid sites that are more active at lower temperature than that of Brønsted ones [112]. Reducing the size of the crystal is another option that has been studied to avoid diffusion problems and is also a strategy to control the product distribution. Yang et al. [113] proved that SAPO-34 zeolites (CHA type structure) with a nanometric crystal size were more resistant to deactivation due to coke deposition. Likewise, Catizzzone et al. [114] have studied nanosized FER-type zeolites, reporting that crystal sizes below 300 nm presented a methanol conversion of 89% and total selectivity to DME at 240 °C, which, together with the higher concentration of Lewis acid sites of ferrierites (which improves catalytic effectiveness) reduce coke deposition due to the smaller crystal size and lower regeneration temperature needed for zeolite recovery, makes them a promising catalyst to methanol dehydration. Regarding the porous structure of zeolites, the narrow and slender microporous structure of many zeolites such as ZSM-5, similar in size to the guest molecule, hinders DME diffusion, thus inhibiting secondary reactions. To overcome diffusion limitations, several approaches have been proposed, the basic strategies being either to shorten the length of the micropores channel or to widen the pore diameter [115], creating hierarchical zeolites that present mesoporosity but minimize the loss in microporosity.

**Table 3.** Zeolite-based catalysts for MeOH dehydration to DME.

Catalyst	T (°C)	MeOH Conversion (%)	DME Selectivity (%)	Ref.
Na modified H-ZSM-5	230	80	100	[106]
Commercial $\gamma$ -Al <sub>2</sub> O <sub>3</sub>	320	80	100	[106]
2-DFER zeolite (Si/Al = 8.4)	240	55	100	[94]
H-Mordenite, MCDH-1	300	84	99	[107]
FER channel system	180	61	95	[103]
MFI channel system	180	30	96	[103]
1-D channels ZSM-22	240	65	98	[108]
Desilicated ZSM-5 (Si/Al = 22.5)	200	86	97	[109]

Wang et al. [116] studied composite zeolites with Beta zeolite cores and Y zeolite polycrystalline shells (BFZ) and overgrowing Beta zeolite on the core Y crystal (FAU-BEA), showing that the acidity (as Lewis/Brønsted ratio) of the composites, and hence their activity and selectivity, can be tuned by controlling the synthesis conditions. In addition, they stated that the increase in methanol conversion could also be due to the composite's unique crystal structure, which facilitated not only mass but also heat transfer in the exothermic reaction of methanol dehydration, as previously reported by Dimitrova et al. [117].

Nonetheless, the porous size is not the only crucial parameter to take into consideration, also channel opening and orientation are key factors in zeolite's catalytic performance. It is widely accepted and supported by DFT and experimental studies that methanol is preferentially adsorbed on 12-membered rings channels than on eight-membered ones [118,119]. Regarding orientation, it has been reported that one-dimensional zeolites such as ZSM-12 (MTW type) or mordenite (MOR) present a remarkable DME selectivity at a low temperature (240 °C), and that those with smaller pores rapidly formed coke deposits, whereas those with medium pore 1-D zeolites like ZSM-22 (TON type) are more resistant to coke deactivation thanks to its particular shape selectivity that inhibits the formation of aromatic species deposits responsible for coke formation [108]. On the other hand, 3-D zeolites like

SAPO-34 or ZSM-5 (MFI type) with similar channel intersection and opening sizes, are less likely to present with coke deactivation and also present high stability and selectivity to DME [94,120].

### 3. Direct Synthesis: CO<sub>2</sub> to DME

Although the DME synthesis from syngas and the obtention via the indirect method, previously described in this review, are widely established in the industry, they present considerable disadvantages: the former method entails the release of CO<sub>2</sub>, that contributes to the greenhouse effect, and the latter involves methanol dehydration, with this being reaction thermodynamically disfavoured [27]. To overcome these limitations, the direct synthesis of DME from CO<sub>2</sub> arises as the most feasible option because it uses CO<sub>2</sub> as a feedstock in the synthesis of DME, a highly valuable product, and also it is a more economical process since all reactions take place jointly and the operating conditions are milder [121].

To carry out the DME direct synthesis, bifunctional catalysts that combines both components are necessary to accomplish methanol synthesis and dehydration. On the one hand, the CO<sub>2</sub> catalytic hydrogenation to produce methanol is a pivotal step in the DME direct synthesis, so the catalysts active in the direct water–gas–shift (WGS) reaction could also be used in the reverse case, given the reversible nature of this reaction, such as CuO–ZnO, and derivatives with Al<sub>2</sub>O<sub>3</sub>, CrO<sub>3</sub> or TiO<sub>2</sub>–ZrO<sub>2</sub> [122–124]. On the other hand,  $\gamma$ -alumina, clays or zeolites of proton and non-proton forms, ferrierite, zeolite-Y or mordenite have been studied as acid catalysts for the methanol dehydration, as mentioned in the previous section devoted to DME indirect synthesis method [55,93,96,97]. HZSM-5 zeolite has been used for direct hydration of CO<sub>2</sub> to DME (Equation (3)) due to its acidic properties. However, other systems, also based on silica (clays, SBA-15 or SiO<sub>2</sub>) and with acidic properties such as zeolites are considered alternatives to the latter and this could be target of future research. However, the direct synthesis of DME from CO<sub>2</sub> has not yet been sufficiently studied. Moreover, most of the research that has been carried out has focused almost exclusively on the use of copper as the active phase.

#### 3.1. Catalysts Based on Pure or Doped Silica

It is known that copper leads to a higher catalytic performance in the CO<sub>2</sub> hydrogenation when it is accompanied by some other metal that acts as a promoter and/or prevents copper sintering. Based on the catalysts used industrially in the synthesis of MeOH and DME from syngas, Wang et al. [125] have studied the effect of Al<sub>2</sub>O<sub>3</sub> on the catalytic performance of the Cu–ZnO–Al<sub>2</sub>O<sub>3</sub>–SiO<sub>2</sub> catalyst in CO<sub>2</sub> hydrogenation to DME. Their results show that when adding alumina to the silica support, a high dispersion of copper species and an increase in surface acidity are observed, since alumina is incorporated into the SiO<sub>2</sub> structure and forms useful acid-base sites for obtaining the ether. They demonstrated that when the alumina content is less than 1.4%, the CO<sub>2</sub> conversion is promoted, and with an alumina content of 4% a better synergistic effect is achieved between the formation of methanol and the active sites of the bifunctional catalyst, achieving an optimal DME selectivity.

The synergistic effect between zirconium and copper has been extensively studied by the group of Atakan et al. [126]. They synthesized a hybrid catalyst incorporating Cu nanoparticles in the porous network of Zr-SBA-15, and to study the influence of the chemical state of the catalysts, they used different silica precursors: tetraethyl orthosilicate (TEOS) or sodium metasilicate (SMS). They also used different methods for the Cu incorporation: infiltration (INF) and evaporation-induced wetness impregnation (EIWI). The synthesis procedure affected both the CO<sub>2</sub> conversion and the product selectivity. Catalysts synthesized by EIWI exhibited a higher selectivity for methanol formation, while catalysts made via INF produced more DME during the CO<sub>2</sub> hydrogenation. A silica-based catalyst synthesized from Si alkoxide precursor and with a higher Zr and acid site contents displayed a higher catalytic activity. They also found that selectivity was affected by medium acid sites, since stronger acid sites are more selective for DME and weaker ones for methanol. Their results showed that the presence of both Cu and Zr ions in the framework improved the adsorption of CO<sub>2</sub> and H<sub>2</sub>, in which Cu controls the chemisorption of H<sub>2</sub> and Zr controls the chemisorption of CO<sub>2</sub> [65]. In another study [127], the same

research group proposed another route for the DME formation, by fixing methoxy-groups. When the methoxy-groups' concentration is low, only methanol is formed, whereas at high concentrations of methoxy-groups, DME is formed. Hengne et al. [128] have used gallium as a promoter for mesoporous silica supported copper catalysts. They reported that adding Ga to a Cu/SiO<sub>2</sub> system increased acidic sites, and improved the Cu reducibility and dispersion, which led to a more active and selective catalyst compared to a Cu/SiO<sub>2</sub> catalyst. The higher acidic strength of Cu-Ga supported by SBA-15 was found to play a key role in the dehydration of MeOH to DME. These researchers have also studied the effect of operating conditions like temperature, contact time and pressure. They found that increasing the temperature from 200 to 250 °C increased CO<sub>2</sub> conversion and DME selectivity, whereas selectivity to methanol decreased. Besides, they reported that longer contact times could lead to an increase in DME selectivity at the expense of MeOH selectivity. Likewise, they also found that increasing the pressure from 1 to 25 bar increased conversion and selectivity to DME.

Regarding the studies with an active phase other than copper, a study carried out by Naik et al. [64] reported a series of Al-MCM-41 catalysts prepared using tetrapropyl ammonium hydroxide (TPAOH) as a co-surfactant, which favors the incorporation of Al species in the framework, modifying the acidic and catalytic properties of the Al-MCM-41 catalyst, and hexadecyltrimethylammonium bromide (CTAB) as the structure-directing agent. Catalysts with different amounts of co-surfactant were investigated in the methanol dehydration and the best (MC-4) was mechanically mixed with a commercial catalyst (MK-121) used in the synthesis of methanol, to produce a bi-functional catalyst for the direct DME synthesis from CO<sub>2</sub>/H<sub>2</sub>. These catalysts were used as dehydration components on bifunctional catalysts. According to their results in the bifunctional catalyst, the MC-4 sample as a superior acidic component because more acidic sites showed better CO<sub>2</sub> conversion, stability and DME selectivity. Table 4 summarizes some of the supported silica-based catalysts studied for direct CO<sub>2</sub> hydrogenation to DME in recent years.

**Table 4.** Silica-based catalysts for direct CO<sub>2</sub> hydrogenation to DME.

Catalyst	T (°C)	P (bar)	Conversion CO <sub>2</sub> (%)	Selectivity (%)		Ref.
				MeOH	DME	
CuGa/SBA-15	250	25	3	71	29	[128]
CuO-ZnO/SBA-15	250	30	8.7	19.5	-	[80]
10Cu/ZnO-SBA-15	250	22.5	12.7	78.4	10	[79]
Cu/ZnO-SBA-15	250	22.5	14.2	92.1	< 3	[79]
20Cu/ZnO-SBA-15	250	22.5	12.1	81.9	< 3	[79]
Cu/ZnO/SBA-15	180	40	7.7	97.3	-	[67]
Mn-Cu/ZnO/SBA-15	180	40	10.5	98.6	-	[67]
Cr-Cu/ZnO/SBA-15	180	40	8.7	97.1	-	[67]
CuO/ZnO/Al <sub>2</sub> O <sub>3</sub> /SiO <sub>2</sub>	260	26	20.2	27.1	-	[76]
CuO/ZnO/Al <sub>2</sub> O <sub>3</sub> /TiO <sub>2</sub>	260	26	16.1	25.3	-	[76]
CuO/ZnO/Al <sub>2</sub> O <sub>3</sub> /SiO <sub>2</sub> -TiO <sub>2</sub>	260	26	40.7	41.2	-	[76]
Cu-Zn-Zr/gel-oxalate	240	30	18	51.2	-	[77]
Cu/SBA-15	180	40	8.6	74.6	-	[78]
Cu/ZnO	180	40	5.7	93.9	-	[78]
Cu/MnO	180	40	1.8	98.8	-	[78]
Cu/ZnO/SBA-15	180	40	7.7	97.3	-	[78]
Cu/MnO/SBA-15	180	40	7.9	87.0	-	[78]
Cu/ZnO/MnO/SBA-15	180	40	10.7	98.0	-	[78]
Cu-ZnO-Al <sub>2</sub> O <sub>3</sub> -SiO <sub>2</sub>	250	30	11	10	40	[125]

### 3.2. Clay Based Catalysts

Currently, studies of clay-materials in the synthesis of DME from CO<sub>2</sub> in one step are very few. Again, copper-based catalysts have been studied extensively in the CO<sub>2</sub> hydrogenation to obtain high value-added products such as DME or MeOH. However, it has not yet been possible to synthesize a copper-containing catalyst that gives rise to a high selectivity towards DME or MeOH, mainly due to the agglomeration that this metal undergoes during the reaction [129,130]. Therefore, much of

the current research are focused on the study of bimetallic and bifunctional catalysts (with acidic and hydrogenation sites) for one-step reactions [131,132]. Small amounts of Fe have been reported to prevent copper agglomeration, inhibit oxidation of surface copper, and thus improve its surface area [131]. Based on this idea, F.C.F. Marcos et al. [133] synthesized bimetallic CuFe and CuCo catalysts supported on a montmorillonite-type clay with aluminum pillars for the CO<sub>2</sub> hydrogenation reaction to obtain methanol and dimethyl ether. In fact, they verified that Fe and Co display a synergistic effect on Cu that increases the surface area of exposed Cu and that it also induced the formation of strong basic sites, something that did not happen with the same monometallic Cu catalyst. Furthermore, with respect to the Cu and CuCo catalysts, Fe increased the presence of acid sites of a mainly weak and medium nature, which favored the selectivity towards DME. However, the basic sites of a medium and strong nature favored selectivity towards methanol, and in this case, the presence of Fe in the catalyst formulation showed greater selectivity towards methanol than towards DME. Still, the CuFe catalyst is more selective to DME than the CuCo catalyst. More recently, A. Kornas et al. [134] have also studied the direct hydrogenation of CO<sub>2</sub> to dimethyl ether with CuO/ZrO<sub>2</sub> catalysts supported on montmorillonite K10 modified with heteropolyacids with Keggin structure (XM<sub>12</sub>O<sub>40</sub><sup>n−</sup>), with X = P and M = W or Mo. The incorporation of metal oxides and heteropolyacids into the K10 clay structure leads to a considerable decrease in the specific surface area, volume and pore size. The authors have reported that the W-containing catalyst was thermally more stable and had a higher concentration of acid sites (mainly of a medium and strong nature) than the Mo catalyst (with medium and weak acidity). With all these catalysts, the CO<sub>2</sub> conversion increased with temperature and selectivity to DME decreased because the RWGS reaction was favored at higher temperatures (higher production of CH<sub>4</sub> and CO, especially). The increased acidity of the clay provided by the heteropolyacids improved the conversion compared to that of the unmodified montmorillonite K10, which had too low a surface concentration of acids sites to completely dehydrate the methanol to DME. Lastly, concerning P-Mo and P-W, the latter more efficiently dehydrated methanol towards DME, due to its higher concentration of acid sites. However, considerable amounts of CO were formed as a by-product. The direct hydrogenation of CO<sub>2</sub> to obtain DME in a single step has been investigated more extensively with acid catalysts based on zeolites, especially HZSM-type and SAPO-type zeolites, as will be discussed in the next section. However, the synthesis of these materials requires a high cost. Seeking to reduce costs and improve the catalytic properties of CuO/ZnO metal phases that are used industrially in the synthesis of DME from syngas, Wang et al. [135] synthesized SAPO-34 from kaolin to prepare various CuO-ZnO catalysts supported on kaolin (k) and SAPO-34-kaolin (Sk). They designed four bifunctional catalysts: CZ/S, CZ/Sk, CZ-k/S, and CZ-k/Sk (C = CuO, Z = ZnO, S = SAPO-34, k = kaolin). From this research, the authors concluded that kaolin produced a significant increase in the specific surface area of SAPO-34, causing it to acquire a lamellar structure in which neither the volume nor the pore size varied. Kaolin also favored a smaller metal oxide particle size compared to samples that did not use kaolin in their formulation. All this, together with the acidity generated by the hydroxyl-groups (P-OH, Si-OH and Si-OH-Al) in Sk catalysts, gave the catalysts greater specificity and also provided them with a greater number of contacts with active sites, which resulted in a better performance with respect to the S catalysts. In addition, the lamellar structure of the Sk catalysts gave them greater volume and pore diameter than the S catalysts, which facilitated the heat dissipation and avoided the coke formation, resulting in a longer catalyst life. Table 5 summarizes some of the clay-based catalysts used for direct CO<sub>2</sub> hydrogenation to dimethyl ether.

**Table 5.** Clay-based catalysts for direct CO<sub>2</sub> hydrogenation to DME.

Catalyst	T (°C)	P (Bar)	CO <sub>2</sub> Conversion (%)	Selectivity (%)				Ref.
				MeOH	DME	CO	CH <sub>4</sub>	
Cu/V-Al PILC <sup>a</sup>	250	40	5	25	23	2	50	[91]
Cu-Ce/V-Al PILC <sup>a</sup>	250	40	6	40	50	1	9	[91]
Cu-Nb/V-Al PILC <sup>a</sup>	250	40	7	47	39	1	13	[91]
(Cu/ZrO <sub>2</sub> ) <sub>NaOH</sub> + K10	240	40	4.4	31.4	11.3	57.1	0.2	[134]
(Cu/ZrO <sub>2</sub> ) <sub>NaOH</sub> + HPW-K10	240	40	4.6	8.9	24.6	66.2	0.3	[134]
(Cu/ZrO <sub>2</sub> ) <sub>NaOH</sub> + HPMo-K10	240	40	5.4	18.5	15.8	64.7	1.0	[134]
(Cu/ZrO <sub>2</sub> ) <sub>citric</sub> + K10	240	40	3.4	43.1	19.2	37.1	0.6	[134]
(Cu/ZrO <sub>2</sub> ) <sub>citric</sub> + HPW-K10	240	40	2.7	14.5	46.5	36.9	2.1	[134]
(Cu/ZrO <sub>2</sub> ) <sub>citric</sub> + HPMo-K10	240	40	2.6	34.2	19.6	39.2	7.1	[134]
CuO-ZnO/SAPO-34	400	30	33.2	-	21.7	8.1	11.3	[135]
CuO-ZnO-kaolin/SAPO-34	400	30	50.4	-	22.3	7.5	12.6	[135]
CuO-ZnO/SAPO-34- kaolin	400	30	41.3	-	21.5	9.3	11.8	[135]
CuO-ZnO-kaolin/SAPO-34- kaolin	400	30	57.6	-	21.4	9.6	11.4	[135]
CuFe/V-Al PILC	250	40	5	23	41	21.5	14	[133]
CuCo/V-Al PILC	250	40	7.5	12.5	19	15	52	[133]

<sup>a</sup> V-Al-PILC: Volclay Al-pillared.

### 3.3. Zeolites Based Catalysts

For the CO<sub>2</sub> direct hydrogenation to DME, zeolites are especially considered given their acidity, negligible sensitivity to water, shape selectivity and high specific surface area [44]. As in the case of catalysts based on clays and mesoporous silicas, the most used active phase with zeolites has been copper. However, as mentioned in previous sections, copper by itself does not achieve entirely satisfactory results, which is the reason why most authors also add other metallic phases in the form of oxides, such as zinc and aluminum. This is the case of the study carried out by Naik et al. [121], who studied two sets of bifunctional catalysts containing 6CuO-3ZnO-Al<sub>2</sub>O<sub>3</sub> (CZA) for the methanol synthesis and  $\gamma$ -alumina or H-ZSM-5 as methanol dehydration catalysts. The hybrid catalyst containing H-ZSM-5 showed a better performance in CO<sub>2</sub> conversion and DME selectivity than the system containing pure Cu. However, the catalyst with  $\gamma$ -alumina showed severe deactivation and detriment when operating in a slurry reactor, due to its hydrothermal instability. Likewise, the zeolite-containing catalyst attained a higher conversion (32%) and selectivity to DME (75%) when operated in a fixed-bed reactor system, as the water removal from the catalyst surface is more effective. The precursors used for the catalyst preparation also play a significant role in the catalytic performance.

Allahyari et al. [136] launched an investigation into a similar catalytic system containing the same components CZA and HZSM-5 derived from different precursors (acetate or nitrate metal salts) prepared by a novel co-precipitation method involving ultrasound. The catalysts were tested under similar conditions to those reported by Naik's et al. [121], but using syngas as feedstock. The synthesized catalyst showed a CO conversion of nearly 60% and DME selectivity of about 52% suggesting that the precursor exerts a significant influence in the catalytic performance since it affects CuO crystallinity.

CuO combined with TiO<sub>2</sub> and/or ZrO<sub>2</sub> mixed oxides and HZSM-5 have also been reported for DME direct synthesis [44]. The use of mixed oxides is preferred to single oxides, since the former present higher specific surface areas and better thermal stabilities [137]. It was stated that the Ti/Zr ratio was decisive in the catalysis, attaining the best catalytic performance with a Ti/Zr atomic ratio of 1/1, with a ca. 16% CO<sub>2</sub> conversion and 48% DME selectivity. The combinations of CuO-ZnO catalytic systems with different types of zeolites have been thoroughly investigated, in order to find a catalytic system that is active, selective and stable. Regarding the latter, ferrierite (FER) and mordenite (MOR) type zeolites have shown remarkable superior activity and stability [114,138] and also an appropriate acidity for the methanol dehydration, related to the high concentration of Lewis acid sites [139]. Bonura et al. [140] have tested the CuO-ZnO system combined with several types of zeolites. In the case of CuO-ZnO combined with an MOR-type zeolite, the CO<sub>2</sub> conversion was ca. 23% with a DME selectivity of 30%, maintained for 90 h on stream, revealing that a lower framework density of

the zeolite structure provides a lower mass transfer limitation and a higher interface area with metal sites. Likewise, it was stated that the CO<sub>2</sub> conversion depends more on the surface acidity than on the surface area of Cu. However, very high acid catalysts are also more prone to deactivation not only by the coke deposition, but also by the loss of weak acid sites due to water presence, that releases Brønsted acid sites during the reaction inducing the sintering of copper particles [141]. Thus, a trade-off between catalytic activity and catalyst deactivation must be achieved. Core-shell structures are also noteworthy, as they allow the separation of reactants, suppress hydrocarbon-producing side reactions, and avoid deactivation. This behaviour is inherent to the structure, since the acid sites for the methanol synthesis are more accessible in the shell and present less resistance to transport and diffusion, as well as prevent deactivation by sintering of Cu species in the core [142]. In this regard, it has been proved that CuO-ZnO-ZrO<sub>2</sub>@SAPO-11 achieves higher CO<sub>2</sub> conversion and DME selectivity than the same components with a hybrid structure obtained by mixing the single components [143]. The authors reported that the best catalytic performance was related to two main facts. On the one hand, the suppression of the pelletization step avoids pore blockage so that the core-shell catalyst presented a higher specific surface area and also increased the availability of acid and metallic sites. On the other hand, the separation of the methanol synthesis and dehydration reactions, which take place in the core and the shell, respectively, favors the catalytic performance and limits water presence in the metallic core. Therefore, methanol is forced to pass through acid sites to diffuse out of the catalyst, enhancing the dehydration reaction that takes place at acid sites [144]. CZA catalysts hybridized with zeolites can also be tuned to rare earth metals, as they are suggested to act as promoters to enhance metal dispersion and as thermal stabilizer [145,146]. Wengui et al. [147] studied the DME synthesis from the CO<sub>2</sub> hydrogenation using a bi-functional La-modified CZA/HZSM-5 catalyst, reporting that an appropriate La addition, around 2 wt%, improved the reducibility and dispersion of the metallic phases due to a decrease in the crystallite size of Cu [148]. Qin et al. [149] tested bifunctional Cu-Fe/HZSM-5 catalysts with 1 wt% La or Ce doping at 3 MPa and 260 °C and showed that Ce doping had a greater effect on smaller crystallite size and reducibility of Cu, and also presented a higher specific surface area than the La-modified catalyst. Cu-Fe-La/HZSM-5 and Cu-Fe-Ce/HZSM-5 improved the CO<sub>2</sub> conversion of the undoped bifunctional catalyst by ca. 40% and 50%, respectively, and the DME selectivity was enhanced by almost 100% with both doped catalysts. The catalysts' stability on stream was also boosted from 6 to 15 h when Ce-modified. The authors suggested that this outstanding catalytic performance was due to the formation of Cu<sup>+</sup> species entering into the CeO<sub>2</sub> lattice, forming a solid solution and decreasing the CuO particle size. Another strategy to boost DME direct synthesis comprises the use of noble metals. Pd has shown a remarkable promoting effect on Cu-ZrO<sub>2</sub> mixed with HZSM-5 catalyst [150]. The experiment, carried out in a fixed-bed reactor at 5 MPa and 250 °C, showed that the Pd-decorated CNT presented an excellent capability to adsorb hydrogen and CO<sub>2</sub>, so that the CO<sub>2</sub> hydrogenation rate was increased up to 26% when both zeolite HZSM-5 and Pd-CNT were present in the catalyst formula. In addition, the combination of both noble and rare earth metals is another approach that is considered to enhance DME direct synthesis. Ruizhi et al. [151] reported that bifunctional Pd/HZSM-5 catalyst could enhance its catalytic performance if CeO<sub>2</sub>-CaO promoters were added. The results indicated that the promoters improved the catalytic activity, avoided the coke deposition and increased the sulphur resistance and, therefore, upgraded the catalyst's stability, thanks to the high acidity and the greater Pd dispersion. It was also suggested that the CaO promoter reduces strong acid sites and weakens CO<sub>2</sub> adsorption. Table 6 summarizes some of the zeolite-based catalysts that have been used for direct CO<sub>2</sub> hydrogenation to dimethyl ether.

**Table 6.** Zeolite-based catalysts for direct CO<sub>2</sub> hydrogenation to DME.

Catalyst	T (°C)	P (Bar)	CO <sub>2</sub> Conversion (%)	Selectivity (%)				Ref.
				MeOH	DME	CO	CH <sub>4</sub>	
CZA/γ-Al <sub>2</sub> O <sub>3</sub>	260	50	15.0	15.0	3.0	82.0	-	[121]
CZA/HZSM-5	260	50	29.0	2.0	65.0	33.0	-	[121]
CuO-TiO <sub>2</sub> -ZrO <sub>2</sub> /HZSM-5	275	30	15.6	13.0	47.5	39.2	-	[44]
CuZnZr-FER	220	30	10.7	14.4	53.2	32.4	-	[142]
CuZnZr-FER	260	30	22.0	14.0	38.5	47.5	-	[142]
CuO-ZnO-ZrO <sub>2</sub> /SAPO-11	275	30	8.7	17.0	80.0	3.0	-	[144]
CuFe/HZSM-5	260	30	12.3	0.9	18.3	30.5	50.3	[149]
CuFeZr/HZSM-5	260	30	17.3	1.9	39.9	21.3	36.9	[149]
CuFeLa/HZSM-5	260	30	17.2	1.5	51.3	30.3	16.9	[149]
CuFeCe/HZSM-5	260	30	18.1	2.1	52.0	25.4	20.5	[149]

#### 4. Conclusions

Due to the environmental problem that involves the emission and accumulation of CO<sub>2</sub> in the atmosphere, the elimination of this gas, either by capturing or using it in some industrial processes, becomes of paramount interest. Thus, the hydrogenation of CO<sub>2</sub> to obtain high value-added chemicals and fuels is doubly significant. However, some crucial issues need to be addressed before applying CO<sub>2</sub> hydrogenation in the industry to make it competitive, such as reducing the cost of hydrogen production, or finding the ideal reaction conditions to obtain high CO<sub>2</sub> conversions and high methanol and dimethyl ether selectivities. Currently, copper-based catalysts are presented as the best approach from a technological point of view. However, they suffer from sintering problems at high temperature and also the influence of the water produced in the reaction process results in low CO<sub>2</sub> conversions. In recent years, a wide variety of active phases and catalytic supports based on silica have been studied, from mesoporous silicas of SBA-15 type, to natural clays or zeolites. According to the investigations carried out to date, it seems that the catalytic behavior of copper improves when the Cu<sup>+</sup>/Cu<sup>2+</sup> ratio increases, and also improves substantially if other metals or oxides (Fe, Zn, Zr, Ga, etc.) are added as promoters. Among the supports used, clays and natural zeolites can be considered as the best alternatives to silica base supports given their low cost, high abundance and, due to their porous structure, the great variety of structural, textural and acid modifications to which they can be subjected, and especially due to their considerable content of alumina in their structure, which is revealed as an essential component in this type of reaction. Properties such as acid strength, controlled by the SiO<sub>2</sub>/Al<sub>2</sub>O<sub>3</sub> ratio, type of acidity, necessary porosity to host the active phases or the high specific surface area, seem essential in the design of an optimal catalyst capable of achieving high conversions of CO<sub>2</sub> in low-temperature and pressure operating conditions.

**Author Contributions:** I.B.-M. researched and wrote about zeolite-based catalysts (Sections 2.3 and 3.3); A.I.-M. researched and wrote about clay based catalysts (Sections 2.2 and 3.2) and also revised the original draft; F.J.F. researched and wrote about silica based catalysts (Sections 2.1 and 3.1); D.B.-P. wrote the introduction and the rest of sections and also organized and revised the original draft preparation; E.R.-C. and E.M. revised the original draft. All authors have read and agreed to the published version of the manuscript.

**Funding:** This research received no external funding.

**Acknowledgments:** The authors would like to acknowledge the Ministerio de Ciencia, Innovación y Universidades of Spain Project RTI2018-099668-B-C22, Junta de Andalucía project UMA18-FEDERJA-126 and FEDER funds for financial support. A.I.M. thanks the Ministry of Economy and Competitiveness for a Ramón y Cajal contract (RyC-2015-17870). D.B.P. thanks the University of Málaga (Spain) for a post-doctoral contract.

**Conflicts of Interest:** The authors declare no conflict of interest.

#### References

- Kawi, S.; Kathiraser, Y. CO<sub>2</sub> as an oxidant for high-temperature reactions. *Front. Energy Res.* **2015**, *3*, 1–17. [CrossRef]
- Havran, V.; Duduković, M.P.; Lo, C.S. Conversion of methane and carbon dioxide to higher value products. *Ind. Eng. Chem. Res.* **2011**, *50*, 7089–7100. [CrossRef]

3. Global Carbon Budget. Available online: <https://www.globalcarbonproject.org/carbonbudget/i> (accessed on 1 June 2020).
4. Global Monitoring Laboratory, Carbon Cycle Greenhouse Gases. Available online: <https://www.esrl.noaa.gov/gmd/ccgg/trends/> (accessed on 1 May 2020).
5. Aresta, M.; Dibenedetto, A.; Quaranta, E. State of the art and perspectives in catalytic processes for CO<sub>2</sub> conversion into chemicals and fuels: The distinctive contribution of chemical catalysis and biotechnology. *J. Catal.* **2016**, *343*, 2–45. [CrossRef]
6. Zhou, P.; Wang, M. Carbon dioxide emissions allocation: A review. *Ecol. Econ.* **2016**, *125*, 47–59. [CrossRef]
7. Irish, J.L.; Sleath, A.; Cialone, M.A.; Knutson, T.R.; Jensen, R.E. Simulations of Hurricane Katrina (2005) under sea level and climate conditions for 1900. *Clim. Chang.* **2014**, *122*, 635–649. [CrossRef]
8. Bobicki, E.R.; Liu, Q.; Xu, Z.; Zeng, H. Carbon capture and storage using alkaline industrial wastes. *Prog. Energy Combust. Sci.* **2012**, *38*, 302–320. [CrossRef]
9. Rahman, F.A.; Aziz, M.M.A.; Saidur, R.; Bakar, W.A.W.A.; Hainin, M.R.; Putrajaya, R.; Hassan, N.A. Pollution to solution: Capture and sequestration of carbon dioxide (CO<sub>2</sub>) and its utilization as a renewable energy source for a sustainable future. *Renew. Sustain. Energy Rev.* **2017**, *71*, 112–126. [CrossRef]
10. Bui, M.; Adjiman, C.S.; Anthony, E.J.; Boston, A.; Brown, S.; Fennell, P.S.; Fuss, S.; Galindo, A.; Hackett, L.A.; Hallett, J.P.; et al. Carbon capture and storage (CCS): The way forward. *Energy Environ. Sci.* **2018**, *11*, 1062–1176. [CrossRef]
11. Goddard, P.B.; Yin, J.; Griffies, S.M.; Zhang, S. An extreme event of sea-level rise along the Northeast coast of North America in 2009–2010. *Nat. Commun.* **2015**, *6*, 1–9. [CrossRef] [PubMed]
12. Soares, J.L.; Moreira, R.F.P.M.; José, H.J.; Grande, C.A.; Rodrigues, A.E. Hydrotalcite materials for carbon dioxide adsorption at high temperatures: Characterization and diffusivity measurements. *Sep. Sci. Technol.* **2004**, *39*, 1989–2010. [CrossRef]
13. Davis, G.W.; Talbot, J.R. Polyesters, fibers. *Encycl. Polym. Sci. Technol.* **2002**, *3*, 678–703.
14. Atanga, M.A.; Rezaei, F.; Jawad, A.; Fitch, M.; Rownaghi, A.A. Oxidative dehydrogenation of propane to propylene with carbon dioxide. *Appl. Catal. B Environ.* **2018**, *220*, 429–445. [CrossRef]
15. Falcinelli, S.; Capriccioli, A.; Pirani, F.; Vecchiocattivi, F.; Stranges, S.; Martì, C.; Nicoziani, A.; Topini, E.; Laganà, A. Methane production by CO<sub>2</sub> hydrogenation reaction with and without solid phase catalysis. *Fuel* **2017**, *209*, 802–811. [CrossRef]
16. Vilarrasa-García, E.; Cecilia, J.A.; María, E.; Moya, O.; Cavalcante, C.L.; Cristina, D.; Azevedo, S. “Low Cost” Pore Expanded SBA-15 Functionalized with Amine Groups Applied to CO<sub>2</sub> Adsorption. *Materials* **2015**, *8*, 2495–2513. [CrossRef]
17. Kumar, P.; With, P.; Srivastava, V.C.; Gläser, R.; Mishra, I.M. Efficient ceria-zirconium oxide catalyst for carbon dioxide conversions: Characterization, catalytic activity and thermodynamic study. *J. Alloys Compd.* **2017**, *696*, 718–726. [CrossRef]
18. Koohestanian, E.; Sadeghi, J.; Mohebbi-Kalhari, D.; Shahraki, F.; Samimi, A. A novel process for CO<sub>2</sub> capture from the flue gases to produce urea and ammonia. *Energy* **2018**, *144*, 279–285. [CrossRef]
19. Visconti, C.G.; Martinelli, M.; Falbo, L.; Infantes-Molina, A.; Lietti, L.; Forzatti, P.; Iaquaniello, G.; Palo, E.; Picutti, B.; Brignoli, F. CO<sub>2</sub> hydrogenation to lower olefins on a high surface area K-promoted bulk Fe-catalyst. *Appl. Catal. B Environ.* **2017**, *200*, 530–542. [CrossRef]
20. Sanz, R.; Calleja, G.; Arencibia, A. Applied Surface Science CO<sub>2</sub> adsorption on branched polyethyleneimine impregnated mesoporous silica SBA-15. *Appl. Surf. Sci.* **2010**, *256*, 5323–5328. [CrossRef]
21. Jia, J.; Qian, C.; Dong, Y.; Li, Y.F.; Wang, H.; Ghossoub, M.; Butler, K.T.; Walsh, A.; Ozin, G.A. Heterogeneous catalytic hydrogenation of CO<sub>2</sub> by metal oxides: Defect engineering-perfecting imperfection. *Chem. Soc. Rev.* **2017**, *46*, 4631–4644. [CrossRef]
22. Saeidi, S.; Amin, N.A.S.; Rahimpour, M.R. Hydrogenation of CO<sub>2</sub> to value-added products—A review and potential future developments. *J. CO<sub>2</sub> Util.* **2014**, *5*, 66–81. [CrossRef]
23. Jalama, K. Carbon dioxide hydrogenation over nickel-, ruthenium-, and copper-based catalysts: Review of kinetics and mechanism. *Catal. Rev. Sci. Eng.* **2017**, *59*, 95–164. [CrossRef]
24. Frusteri, F.; Migliori, M.; Cannilla, C.; Frusteri, L.; Catizzone, E.; Aloise, A.; Giordano, G.; Bonura, G. Direct CO<sub>2</sub> to DME hydrogenation reaction: New evidences of a superior behaviour of FER-based hybrid systems to obtain high DME yield. *J. CO<sub>2</sub> Util.* **2017**, *18*, 353–361. [CrossRef]

25. Ateka, A.; Pérez-Uriarte, P.; Gamero, M.; Ereña, J.; Aguayo, A.T.; Bilbao, J. A comparative thermodynamic study on the CO<sub>2</sub> conversion in the synthesis of methanol and of DME. *Energy* **2017**, *120*, 796–804. [CrossRef]
26. Mahmud, A.; Wu, T.; Li, S.; Miles, N.; Mujtaba, I.M. Bio-DME production based on conventional and CO<sub>2</sub> enhanced gasification of biomass: A comparative study on exergy and environmental impacts. *Biomass Bioenergy* **2018**, *110*, 105–113.
27. Chen, W.-H.; Hsu, C.-L.; Wang, X.-D. Thermodynamic approach and comparison of two-step and single step DME (dimethyl ether) syntheses with carbon dioxide utilization. *Energy* **2016**, *109*, 326–340. [CrossRef]
28. IHS Markit, Methanol: Process Economics Program Report. 2019. Available online: <https://ihsmarkit.com/products/chemical-technology-pep-report-43f-methanol.html> (accessed on 1 May 2020).
29. Santos, B.A.V.; Loureiro, J.M.; Ribeiro, A.M.; Rodrigues, A.E.; Cunha, A.F. Methanol production by bi-reforming. *Can. J. Chem. Eng.* **2015**, *93*, 510–526. [CrossRef]
30. Olah, G.A. Towards oil independence through renewable methanol chemistry. *Angew. Chemie Int. Ed.* **2013**, *52*, 104–107. [CrossRef]
31. Kiss, A.A.; Pragt, J.J.; Vos, H.J.; Bargeman, G.; de Groot, M.T. Novel efficient process for methanol synthesis by CO<sub>2</sub> hydrogenation. *Chem. Eng. J.* **2016**, *284*, 260–269. [CrossRef]
32. Din, I.U.; Shaharun, M.S.; Alotaibi, M.A.; Alharthi, A.I.; Naeem, A. Recent developments on heterogeneous catalytic CO<sub>2</sub> reduction to methanol. *J. CO<sub>2</sub> Util.* **2019**, *34*, 20–33. [CrossRef]
33. Azizi, Z.; Rezaeimanesh, M.; Tohidian, T.; Rahimpour, M.R. Dimethyl ether: A review of technologies and production challenges. *Chem. Eng. Process. Process Intensif.* **2014**, *82*, 150–172. [CrossRef]
34. Johnson, D. Global Methanol Market Review, IHS Inc. 2012. Available online: <http://www.ptq.pemex.com/productosyservicios/eventosdescargas/Documents/Foro> (accessed on 1 June 2020).
35. Ahmad, R.; Dinjus, E.; Sauer, J.; Arnold, U. The single step process for the synthesis of DME from biomass-derived syngas. In Proceedings of the Ruaa Ahmad-1. International TMFB-Conference, Aachen, Germany, 18–20 June 2010; pp. 1–28. Available online: [https://www.rwth-aachen.de/global/show\\_document.asp?id=aaaaaaaaaynujm](https://www.rwth-aachen.de/global/show_document.asp?id=aaaaaaaaaynujm) (accessed on 1 July 2020).
36. Methanol Institute. Available online: <http://www.methanol.org/wp-content/uploads/2016/06/DME-An-Emerging-Global-Guel-FS.pdf> (accessed on 1 July 2020).
37. Han, S.; Sik, C. Applicability of dimethyl ether (DME) in a compression ignition engine as an alternative fuel. *Energy Convers. Manag.* **2014**, *86*, 848–863.
38. Papari, S.; Kazemeini, M.; Fattahi, M. Modelling-based optimisation of the direct synthesis of dimethyl ether from syngas in a commercial slurry reactor. *Chin. J. Chem. Eng.* **2013**, *21*, 611–621. [CrossRef]
39. Cheng, C.; Zhang, H.; Ying, W.; Fang, D. Intrinsic kinetics of one-step dimethyl ether synthesis from hydrogen-rich synthesis gas over bi-functional catalyst. *Korean J. Chem. Eng.* **2011**, *28*, 1511–1517. [CrossRef]
40. Trippe, F.; Fröhling, M.; Schultmann, F.; Stahl, R.; Henrich, E.; Dalai, A. Comprehensive techno-economic assessment of dimethyl ether (DME) synthesis and Fischer-Tropsch synthesis as alternative process steps within biomass to liquid production. *Fuel Process. Technol.* **2013**, *106*, 577–586. [CrossRef]
41. Arcoumanis, C.; Bae, C.; Crookes, R.; Kinoshita, E. The potential of dimethyl ether (DME) as an alternative fuel for compression-ignition engines: A review. *Fuel* **2008**, *87*, 1014–1030. [CrossRef]
42. Yaripour, F.; Baghaei, F.; Schmidt, I.; Perregaard, J. Catalytic dehydration of methanol to dimethyl ether (DME) over solid-acid catalysts. *Catal. Commun.* **2005**, *6*, 147–152. [CrossRef]
43. de Carvalho, E.; Silva, D.F. *DME as Alternative Diesel Fuel: Overview*; SAE Technical Paper; SAE: Warrendale, PA, USA, 2006. [CrossRef]
44. Wang, S.; Mao, D.; Guo, X.; Wu, G.; Lu, G. Dimethyl ether synthesis via CO<sub>2</sub> hydrogenation over CuO–TiO<sub>2</sub>–ZrO<sub>2</sub>/HZSM-5 bifunctional catalysts. *Catal. Commun.* **2009**, *10*, 1367–1370. [CrossRef]
45. Frusteri, F.; Cordaro, M.; Cannilla, C.; Bonura, G. Multifunctionality of Cu–ZnO–ZrO<sub>2</sub>/H-ZSM5 catalysts for the one-step CO<sub>2</sub> to DME hydrogenation reaction. *Appl. Catal. B Environ.* **2015**, *162*, 57–65. [CrossRef]
46. Zhou, X.; Su, T.; Jiang, Y.; Qin, Z.; Ji, H.; Guo, Z. CuO–Fe<sub>2</sub>O<sub>3</sub>–CeO<sub>2</sub>/HZSM-5 bifunctional catalyst hydrogenated CO<sub>2</sub> for enhanced dimethyl ether synthesis. *Chem. Eng. Sci.* **2016**, *153*, 10–20. [CrossRef]
47. Ahn, N.H.; Seo, S.; Hong, S.B. Small-pore molecular sieves SAPO-57 and SAPO-59: Synthesis, characterization, and catalytic properties in methanol to olefins conversion. *Catal. Sci. Technol.* **2016**, *6*, 2725–2734. [CrossRef]
48. Oyola-Rivera, O.; Baltanás, M.A.; Cardona-Martínez, N. CO<sub>2</sub> hydrogenation to methanol and dimethyl ether by Pd–Pd<sub>2</sub>Ga catalysts supported over Ga<sub>2</sub>O<sub>3</sub> polymorphs. *J. CO<sub>2</sub> Util.* **2015**, *9*, 8–15. [CrossRef]

49. Fan, Y.J.; Wu, S.F. A graphene-supported copper-based catalyst for the hydrogenation of carbon dioxide to form methanol. *J. CO<sub>2</sub> Util.* **2016**, *16*, 150–156. [[CrossRef](#)]
50. Jadhav, S.G.; Vaidya, P.D.; Bhanage, B.M.; Joshi, J.B. Catalytic carbon dioxide hydrogenation to methanol: A review of recent studies. *Chem. Eng. Res. Des.* **2014**, *92*, 2557–2567. [[CrossRef](#)]
51. Wu, J.; Saito, M.; Takeuchi, M.; Watanabe, T. The stability of Cu/ZnO-based catalysts in methanol synthesis from a CO<sub>2</sub>-rich feed and from a CO-rich feed. *Appl. Catal. A Gen.* **2001**, *218*, 235–240. [[CrossRef](#)]
52. Gao, Z.; Huang, W.; Yin, L.; Xie, K. Liquid-phase preparation of catalysts used in slurry reactors to synthesize dimethyl ether from syngas: Effect of heat-treatment atmosphere. *Fuel Process. Technol.* **2009**, *90*, 1442–1446. [[CrossRef](#)]
53. Suh, Y.W.; Moon, S.H.; Rhee, H.K. Active sites in Cu/ZnO/ZrO<sub>2</sub> catalysts for methanol synthesis from CO/H<sub>2</sub>. *Catal. Today* **2000**, *63*, 447–452. [[CrossRef](#)]
54. Sun, K.; Lu, W.; Qiu, F.; Liu, S.; Xu, X. Direct synthesis of DME over bifunctional catalyst: Surface properties and catalytic performance. *Appl. Catal. A Gen.* **2003**, *252*, 243–249. [[CrossRef](#)]
55. Bahmanpour, A.M.; Héroguel, F.; Baranowski, C.J.; Luterbacher, J.S.; Kröcher, O. Selective synthesis of dimethyl ether on eco-friendly K10 montmorillonite clay. *Appl. Catal. A Gen.* **2018**, *560*, 165–170. [[CrossRef](#)]
56. Zheng, J.; Zeng, Q.; Yi, Y.; Wang, Y.; Ma, J.; Qin, B.; Zhang, X.; Sun, W.; Li, R. The hierarchical effects of zeolite composites in catalysis. *Catal. Today* **2011**, *168*, 124–132. [[CrossRef](#)]
57. Rownaghi, A.A.; Rezaei, F.; Stante, M.; Hedlund, J. Selective dehydration of methanol to dimethyl ether on ZSM-5 nanocrystals. *Appl. Catal. B Environ.* **2012**, *119–120*, 56–61. [[CrossRef](#)]
58. Dębek, R.; Ribeiro, M.F.G.; Fernandes, A.; Motak, M. Dehydration of methanol to dimethyl ether over modified vermiculites. *Comptes Rendus Chim.* **2015**, *18*, 1211–1222. [[CrossRef](#)]
59. Marosz, M.; Kowalczyk, A.; Gil, B.; Chmielarz, L. Acid-treated clay minerals as catalysts for dehydration of methanol and ethanol. *Clays Clay Miner.* **2020**, *68*, 23–37. [[CrossRef](#)]
60. Ramos, F.S.; De Farias, A.M.D.; Borges, L.E.P.; Monteiro, J.L.; Fraga, M.A.; Sousa-Aguiar, E.F.; Appel, L.G. Role of dehydration catalyst acid properties on one-step DME synthesis over physical mixtures. *Catal. Today* **2005**, *101*, 39–44. [[CrossRef](#)]
61. Khaleel, A. Titanium-doped alumina for catalytic dehydration of methanol to dimethyl ether at relatively low temperatures. *Fuel* **2011**, *90*, 2422–2427. [[CrossRef](#)]
62. Union, I.; Pure, O.F.; Chemistry, A. Recommendations for the characterization of porous solids. *Pure Appl. Chem.* **1994**, *66*, 1739–1758.
63. Ciftci, A.; Varisli, D.; Dogu, T. Dimethyl Ether Synthesis over Novel Silicotungstic Acid Incorporated Nanostructured Catalysts. *Int. J. Chem.* **2010**, *8*. [[CrossRef](#)]
64. Naik, S.P.; Bui, V.; Ryu, T.; Miller, J.D.; Zmierczak, W. Al-MCM-41 as methanol dehydration catalyst. *Appl. Catal. A Gen.* **2010**, *381*, 183–190. [[CrossRef](#)]
65. Atakan, A.; Mäkie, P.; Söderlind, F.; Keraudy, J.; Björk, E.M.; Odén, M. Synthesis of a Cu-infiltrated Zr-doped SBA-15 catalyst for CO<sub>2</sub> hydrogenation into methanol and dimethyl ether. *Phys. Chem. Chem. Phys.* **2017**, *19*, 19139–19149. [[CrossRef](#)]
66. Tang, Q.; Xu, H.; Zheng, Y.; Wang, J.; Li, H.; Zhang, J. Catalytic dehydration of methanol to dimethyl ether over micro-mesoporous ZSM-5/MCM-41 composite molecular sieves. *Appl. Catal. A Gen.* **2012**, *413–414*, 36–42. [[CrossRef](#)]
67. Koh, M.K.; Zain, M.M.; Mohamed, A.R. Exploring transition metal (Cr, Mn, Fe, Co, Ni) promoted copper-catalyst for carbon dioxide hydrogenation to methanol. *AIP Conf. Proc.* **2019**, *2124*. [[CrossRef](#)]
68. Sang, Y.; Li, H.; Zhu, M.; Ma, K.; Jiao, Q.; Wu, Q. Catalytic performance of metal ion doped MCM-41 for methanol dehydration to dimethyl ether. *J. Porous Mater.* **2013**, *20*, 1509–1518. [[CrossRef](#)]
69. Brodie-Linder, N.; Dosseh, G.; Alba-Simonesco, C.; Audonnet, F.; Impérator-Clerc, M. SBA-15 synthesis: Are there lasting effects of temperature change within the first 10 min of TEOS polymerization? *Mater. Chem. Phys.* **2008**, *108*, 73–81. [[CrossRef](#)]
70. Johansson, E.M.; Córdoba, J.M.; Odén, M. The effects on pore size and particle morphology of heptane additions to the synthesis of mesoporous silica SBA-15. *Microporous Mesoporous Mater.* **2010**, *133*, 66–74. [[CrossRef](#)]
71. Johansson, E.M.; Ballem, M.A.; Córdoba, J.M.; Odén, M. Rapid synthesis of SBA-15 rods with variable lengths, widths, and tunable large pores. *Langmuir* **2011**, *27*, 4994–4999. [[CrossRef](#)]

72. Herrera, J.E.; Kwak, J.H.; Hu, J.Z.; Wang, Y.; Peden, C.H.F.; MacHt, J.; Iglesia, E. Synthesis, characterization, and catalytic function of novel highly dispersed tungsten oxide catalysts on mesoporous silica. *J. Catal.* **2006**, *239*, 200–211. [[CrossRef](#)]
73. Benitez, V.M.; Querini, C.A.; Fô, N.S. Skeletal isomerization of 1-butene on  $\text{WO}_x/\text{g-Al}_2\text{O}_3$ . *Appl. Catal. A Gen.* **1999**, *178*. [[CrossRef](#)]
74. Carniti, P.; Gervasini, A.; Auroux, A. Energy distribution of surface acid sites of metal oxides. *J. Catal.* **1994**, *150*, 274–283. [[CrossRef](#)]
75. Bernholc, J.; Horsley, J.A.; Murrell, L.L.; Sherman, L.G.; Soled, S. Brønsted acid sites in transition metal oxide catalysts: Modeling of structure, acid strengths, and support effects. *J. Phys. Chem.* **1987**, *91*, 1526–1530. [[CrossRef](#)]
76. Zhang, L.; Zhang, Y.; Chen, S. Effect of promoter  $\text{SiO}_2$ ,  $\text{TiO}_2$  or  $\text{SiO}_2\text{-TiO}_2$  on the performance of  $\text{CuO-ZnO-Al}_2\text{O}_3$  catalyst for methanol synthesis from  $\text{CO}_2$  hydrogenation. *Appl. Catal. A Gen.* **2012**, *415–416*, 118–123. [[CrossRef](#)]
77. Bonura, G.; Cordaro, M.; Cannilla, C.; Arena, F.; Frusteri, F. The changing nature of the active site of Cu-Zn-Zr catalysts for the  $\text{CO}_2$  hydrogenation reaction to methanol. *Appl. Catal. B Environ.* **2014**, *152–153*, 152–161. [[CrossRef](#)]
78. Koh, M.K.; Wong, Y.J.; Chai, S.P.; Mohamed, A.R. Carbon dioxide hydrogenation to methanol over multi-functional catalyst: Effects of reactants adsorption and metal-oxide(s) interfacial area. *J. Ind. Eng. Chem.* **2018**, *62*, 156–165. [[CrossRef](#)]
79. Tasfy, S.F.H.; Zabidi, N.A.M.; Shaharun, M.S.; Subbarao, D.; Elbagir, A. Carbon dioxide hydrogenation to methanol over Cu/ZnO-SBA-15 catalyst: Effect of metal loading. *Defect Diffus. Forum.* **2017**, *380*, 151–160. [[CrossRef](#)]
80. Lin, M.; Na, W.; Ye, H.C.; Huo, H.H.; Gao, W.G. Effect of additive on CuO-ZnO/SBA-15 catalytic performance of  $\text{CO}_2$  hydrogenation to methanol. *Ranliao Huaxue Xuebao J. Fuel Chem. Technol.* **2019**, *47*, 1214–1225. [[CrossRef](#)]
81. Elfadly, A.M.; Zeid, I.F.; Yehia, F.Z.; Abouelela, M.M.; Rabie, A.M. Production of aromatic hydrocarbons from catalytic pyrolysis of lignin over acid-activated bentonite clay. *Fuel Process. Technol.* **2017**, *163*, 1–7. [[CrossRef](#)]
82. Li, K.; Lei, J.; Yuan, G.; Weerachanchai, P.; Wang, J.Y.; Zhao, J.; Yang, Y. Fe-, Ti-, Zr- and Al-pillared clays for efficient catalytic pyrolysis of mixed plastics. *Chem. Eng. J.* **2017**, *317*, 800–809. [[CrossRef](#)]
83. Han, J.; Wang, T.; Feng, S.; Li, C.; Zhang, Z. One-pot synthesis of 3-(furan-2-yl)-4: H -chromen-4-ones from 1-(2-hydroxyphenyl)butane-1,3-diones and 2,5-dimethoxy-2,5-dihydrofuran catalyzed via K10 montmorillonite under solvent-free conditions. *Green Chem.* **2016**, *18*, 4092–4097. [[CrossRef](#)]
84. Soni, V.K.; Sharma, R.K. Palladium-nanoparticles-intercalated montmorillonite clay: A green catalyst for the solvent-free chemoselective hydrogenation of squalene. *ChemCatChem* **2016**, *8*, 1763–1768. [[CrossRef](#)]
85. Chaisena, A.; Rangsiwatananon, K. Synthesis of sodium zeolites from natural and modified diatomite. *Mater. Lett.* **2005**, *59*, 1474–1479. [[CrossRef](#)]
86. Bieseki, L.; Bertella, F.; Treichel, H.; Penha, F.G.; Pergher, S.B.C. Acid treatments of montmorillonite-rich clay for Fe removal using a factorial design method. *Mater. Res.* **2013**, *16*, 1122–1127. [[CrossRef](#)]
87. Colina, F.G.; Llorens, J. Study of the dissolution of dealuminated kaolin in sodium-potassium hydroxide during the gel formation step in zeolite X synthesis. *Microporous Mesoporous Mater.* **2007**, *100*, 302–311. [[CrossRef](#)]
88. Pranee, W.; Neramittagapong, S.; Assawasaengrat, P.; Neramittagapong, A. Methanol dehydration to dimethyl ether over strong-acid-modified diatomite catalysts. *Energy Sources Part A Recover. Util. Environ. Eff.* **2016**, *38*, 3109–3115. [[CrossRef](#)]
89. Hashimoto, K.; Hanada, Y.; Minami, Y.; Kera, Y. Conversion of methanol to dimethyl ether and formaldehyde over alumina intercalated in a montmorillonite. *Appl. Catal. A Gen.* **1996**, *141*, 57–69. [[CrossRef](#)]
90. Chmielarz, L.; Kowalczyk, A.; Skoczek, M.; Rutkowska, M.; Gil, B.; Natkański, P.; Radko, M.; Motak, M.; Dębek, R.; Ryzkowski, J. Porous clay heterostructures intercalated with multicomponent pillars as catalysts for dehydration of alcohols. *Appl. Clay Sci.* **2018**, *160*, 116–125. [[CrossRef](#)]
91. Marcos, F.C.F.; Assaf, J.M.; Assaf, E.M. Catalytic hydrogenation of  $\text{CO}_2$  into methanol and dimethyl ether over Cu-X/V-Al PILC (X = Ce and Nb) catalysts. *Catal. Today* **2017**, *289*, 173–180. [[CrossRef](#)]
92. Marosz, M.; Kowalczyk, A.; Chmielarz, L. Modified vermiculites as effective catalysts for dehydration of methanol and ethanol. *Catal. Today* **2019**, 1–10. [[CrossRef](#)]
93. Xu, M.; Lunsford, J.H.; Goodman, D.W.; Bhattacharyya, A. Synthesis of dimethyl ether (DME) from methanol over solid-acid catalysts. *Appl. Catal. A Gen.* **1997**, *149*, 289–301. [[CrossRef](#)]

94. Catizzzone, E.; Aloise, A.; Migliori, M.; Giordano, G. From 1-D to 3-D zeolite structures: Performance assessment in catalysis of vapour-phase methanol dehydration to DME. *Microporous Mesoporous Mater.* **2017**, *243*, 102–111. [\[CrossRef\]](#)
95. Alaba, P.A.; Abbas, A.; Daud, W.M.W. Insight into catalytic reduction of CO<sub>2</sub>: Catalysis and reactor design. *J. Clean. Prod.* **2017**, *140*, 1298–1312. [\[CrossRef\]](#)
96. Alharbi, W.; Kozhevnikova, E.F.; Kozhevnikov, I.V. Dehydration of methanol to dimethyl ether over heteropoly acid catalysts: The relationship between reaction rate and catalyst acid strength. *ACS Catal.* **2015**, *5*, 7186–7193. [\[CrossRef\]](#)
97. Ortega, C.; Rezaei, M.; Hessel, V.; Kolb, G. Methanol to dimethyl ether conversion over a ZSM-5 catalyst: Intrinsic kinetic study on an external recycle reactor. *Chem. Eng. J.* **2018**, *347*, 741–753. [\[CrossRef\]](#)
98. Chen, Z.; Li, X.; Xu, Y.; Dong, Y.; Lai, W.; Fang, W.; Yi, X. Fabrication of nano-sized SAPO-11 crystals with enhanced dehydration of methanol to dimethyl ether. *Catal. Commun.* **2018**, *103*, 1–4. [\[CrossRef\]](#)
99. Martínez, C.; Corma, A. Zeolites. *Compr. Inorg. Chem. II* **2013**, *5*, 103–131.
100. Guisnet, M.; Magnoux, P. Deactivation of zeolites by coking. Prevention of deactivation and regeneration. In *Zeolite Microporous Solids: Synthesis, Structure, and Reactivity*; Springer: Dordrecht, The Netherlands, 1992; pp. 457–474. [\[CrossRef\]](#)
101. Hassanpour, S.; Taghizadeh, M.; Yaripour, F. Preparation, characterization, and activity evaluation of H-ZSM-5 catalysts in vapor-phase methanol dehydration to dimethyl ether. *Ind. Eng. Chem. Res.* **2010**, *49*, 4063–4069. [\[CrossRef\]](#)
102. Khandan, N.; Kazemeini, M.; Aghaziarati, M. Aghaziarati, dehydration of methanol to dimethyl ether employing modified H-ZSM-5 catalysts. *Iran. J. Chem. Eng.* **2009**, *6*, 1.
103. Migliori, M.; Catizzzone, E.; Aloise, A.; Bonura, G.; Gómez-Hortigüela, L.; Frusteri, L.; Cannilla, C.; Frusteri, F.; Giordano, G. New insights about coke deposition in methanol-to-DME reaction over MOR-, MFI- and FER-type zeolites. *J. Ind. Eng. Chem.* **2018**, *68*, 196–208. [\[CrossRef\]](#)
104. Wan, Z.; Li, G.K.; Wang, C.; Yang, H.; Zhang, D. Relating coke formation and characteristics to deactivation of ZSM-5 zeolite in methanol to gasoline conversion. *Appl. Catal. A Gen.* **2018**, *549*, 141–151. [\[CrossRef\]](#)
105. Guisnet, M.; Magnoux, P. Deactivation by coking of zeolite catalysts. Prevention of deactivation. Optimal conditions for regeneration. *Catal. Today* **1997**, *36*, 477–483. [\[CrossRef\]](#)
106. Vishwanathan, V.; Jun, K.-W.; Kim, J.-W.; Roh, H.-S. Vapour phase dehydration of crude methanol to dimethylether over Na modified H-ZSM-5 catalysts. *Appl. Catal. A Gen.* **2004**, *276*, 251–255. [\[CrossRef\]](#)
107. Moradi, G.R.; Yaripour, F.; Vale-Sheyda, P. Catalytic dehydration of methanol to dimethyl ether over mordenite catalysts. *Fuel Process. Technol.* **2010**, *91*, 461–468. [\[CrossRef\]](#)
108. Catizzzone, E.; Cirelli, Z.; Aloise, A.; Lanzafame, P.; Migliori, M.; Giordano, G. Methanol conversion over ZSM-12, ZSM-22 and EU-1 zeolites: From DME to hydrocarbons production. *Catal. Today* **2018**, *304*, 39–50. [\[CrossRef\]](#)
109. Aloise, A.; Marino, A.; Dalena, F.; Giorgianni, G.; Migliori, M.; Frusteri, L.; Cannilla, C.; Bonura, G.; Frusteri, F.; Giordano, G. Desilicated ZSM-5 zeolite: Catalytic performances assessment in methanol to DME dehydration. *Microporous Mesoporous Mater.* **2020**, *302*, 110198. [\[CrossRef\]](#)
110. Cejka, J.; van Bekkum, H. *Zeolites and ordered Mesoporous Materials: Progress and Prospects. The 1st FEZA School on Zeolites, Prague, Czech Republic, 20–21 August 2005*; Elsevier: Amsterdam, The Netherlands, 2005; ISBN 9780080457338.
111. Kianfar, E.; Hajimirzaee, S.; Mousavian, S.; Mehr, A.S. Zeolite-based catalysts for methanol to gasoline process: A review. *Microchem. J.* **2020**, *156*, 104822. [\[CrossRef\]](#)
112. Hu, Y.; Nie, Z.; Fang, D. Simulation and model design of pipe-shell reactor for the direct synthesis of dimethyl ether from syngas. *J. Nat. Gas Chem.* **2008**, *17*, 195–200. [\[CrossRef\]](#)
113. Yang, G.; Wei, Y.; Xu, S.; Chen, J.; Li, J.; Liu, Z.; Yu, J.; Xu, R. Nanosize enhanced lifetime of SAPO-34 catalysts in methanol to olefin reactions. *J. Phys. Chem. C* **2013**, *117*, 8214–8222. [\[CrossRef\]](#)
114. Catizzzone, E.; Van Daele, S.; Bianco, M.; Di Michele, A.; Aloise, A.; Migliori, M.; Valtchev, V.; Giordano, G. Catalytic application of ferrierite nanocrystals in vapour-phase dehydration of methanol to dimethyl ether. *Appl. Catal. B Environ.* **2019**, *243*, 273–282. [\[CrossRef\]](#)
115. Pérez-Ramírez, J.; Christensen, C.H.; Egeblad, K.; Christensen, C.H.; Groen, J.C. Hierarchical zeolites: Enhanced utilisation of microporous crystals in catalysis by advances in materials design. *Chem. Soc. Rev.* **2008**, *37*, 2530–2542. [\[CrossRef\]](#)

116. Wang, Y.; Wang, W.L.; Chen, Y.X.; Zheng, J.J.; Li, R.F. Synthesis of dimethyl ether from syngas using a hierarchically porous composite zeolite as the methanol dehydration catalyst. *Ranliao Huaxue Xuebao J. Fuel Chem. Technol.* **2013**, *41*, 875–882. [\[CrossRef\]](#)
117. Dimitrova, R.; Gunduz, G.; Dimitrov, L.; Tsoncheva, T.; Yilmaz, S.; Urqueta-Gonzalez, E.A. Acidic sites in beta zeolites in dependence of the preparation methods. *J. Mol. Catal. A Chem.* **2004**, *214*, 265–268. [\[CrossRef\]](#)
118. Masudi, A.; Jusoh, N.W.C.; Muraza, O. Opportunities for less-explored zeolitic materials in the syngas to olefins pathway over nanoarchitected catalysts: A mini review. *Catal. Sci. Technol.* **2020**, *10*, 1582–1596. [\[CrossRef\]](#)
119. Gong, K.; Jiao, F.; Chen, Y.; Liu, X.; Pan, X.; Han, X.; Bao, X.; Hou, G. Insights into the site-selective adsorption of methanol and water in mordenite zeolite by  $^{129}\text{Xe}$  NMR spectroscopy. *J. Phys. Chem. C* **2019**, *123*, 17368–17374. [\[CrossRef\]](#)
120. Mondal, U.; Yadav, G.D. Perspective of dimethyl ether as fuel: Part I—Catalysis. *J. CO<sub>2</sub> Util.* **2019**, *32*, 299–320. [\[CrossRef\]](#)
121. Naik, S.P.; Ryu, T.; Bui, V.; Miller, J.D.; Drinnan, N.B.; Zmierczak, W. Synthesis of DME from CO<sub>2</sub>/H<sub>2</sub> gas mixture. *Chem. Eng. J.* **2011**, *167*, 362–368. [\[CrossRef\]](#)
122. Fierro, J.L.G.; Melián-Cabrera, I.; López Granados, M. Reverse topotactic transformation of a Cu-Zn-Al catalyst during wet Pd impregnation: Relevance for the performance in methanol synthesis from CO<sub>2</sub>/H<sub>2</sub> mixtures. *J. Catal.* **2002**, *210*, 273–284.
123. Zhang, X.R.; Wang, L.C.; Yao, C.Z.; Cao, Y.; Dai, W.L.; He, H.Y.; Fan, K.N. A highly efficient Cu/ZnO/Al<sub>2</sub>O<sub>3</sub> catalyst via gel-coprecipitation of oxalate precursors for low-temperature steam reforming of methanol. *Catal. Lett.* **2005**, *102*, 183–190. [\[CrossRef\]](#)
124. Hirano, M.; Yasutake, T.; Kuroda, K. Dimethyl ether synthesis from carbon dioxide by catalytic hydrogenation (Part 3) direct synthesis using hybrid catalyst by recycling process. *J. Jpn. Pet. Inst.* **2005**, *48*, 197–203. [\[CrossRef\]](#)
125. Wang, J.; Zeng, C. Al<sub>2</sub>O<sub>3</sub> Effect on the catalytic activity of Cu-ZnO-Al<sub>2</sub>O<sub>3</sub>-SiO<sub>2</sub> catalysts for dimethyl ether synthesis from CO<sub>2</sub> hydrogenation. *J. Nat. Gas Chem.* **2005**, *14*, 156–162.
126. Atakan, A.; Keraudy, J.; Mäkie, P.; Hultberg, C.; Björk, E.M.; Odén, M. Impact of the morphological and chemical properties of copper-zirconium-SBA-15 catalysts on the conversion and selectivity in carbon dioxide hydrogenation. *J. Colloid Interface Sci.* **2019**, *546*, 163–173. [\[CrossRef\]](#)
127. Atakan, A.; Erdtman, E.; Mäkie, P.; Ojamäe, L.; Odén, M. Time evolution of the CO<sub>2</sub> hydrogenation to fuels over Cu-Zr-SBA-15 catalysts. *J. Catal.* **2018**, *362*, 55–64. [\[CrossRef\]](#)
128. Hengne, A.M.; Bhatte, K.D.; Ould-Chikh, S.; Saih, Y.; Basset, J.M.; Huang, K.W. Selective production of oxygenates from carbon dioxide hydrogenation over a mesoporous-silica-supported copper-gallium nanocomposite catalyst. *ChemCatChem* **2018**, *10*, 1360–1369. [\[CrossRef\]](#)
129. Xie, Q.; Chen, P.; Peng, P.; Liu, S.; Peng, P.; Zhang, B.; Cheng, Y.; Wan, Y.; Liu, Y.; Ruan, R. Single-step synthesis of DME from syngas on CuZnAl-zeolite bifunctional catalysts: The influence of zeolite type. *RSC Adv.* **2015**, *5*, 26301–26307. [\[CrossRef\]](#)
130. Rodriguez, J.A.; Liu, P.; Stacchiola, D.J.; Senanayake, S.D.; White, M.G.; Chen, J.G. Hydrogenation of CO<sub>2</sub> to Methanol: Importance of Metal-Oxide and Metal-Carbide Interfaces in the Activation of CO<sub>2</sub>. *ACS Catal.* **2015**, *5*, 6696–6706. [\[CrossRef\]](#)
131. Xiao, K.; Qi, X.; Bao, Z.; Wang, X.; Zhong, L.; Fang, K.; Lin, M.; Sun, Y. CuFe, CuCo and CuNi nanoparticles as catalysts for higher alcohol synthesis from syngas: A comparative study. *Catal. Sci. Technol.* **2013**, *3*, 1591–1602. [\[CrossRef\]](#)
132. Liu, R.W.; Qin, Z.Z.; Ji, H.B.; Su, T.M. Synthesis of dimethyl ether from CO<sub>2</sub> and H<sub>2</sub> using a Cu-Fe-Zr/HZSM-5 catalyst system. *Ind. Eng. Chem. Res.* **2013**, *52*, 16648–16655. [\[CrossRef\]](#)
133. Marcos, F.C.F.; Assaf, J.M.; Assaf, E.M. CuFe and CuCo supported on pillared clay as catalysts for CO<sub>2</sub> hydrogenation into value-added products in one-step. *Mol. Catal.* **2018**, *458*, 297–306. [\[CrossRef\]](#)
134. Kornas, A.; Śliwa, M.; Ruggiero-Mikołajczyk, M.; Samson, K.; Podobniński, J.; Karcz, R.; Duraczyńska, D.; Rutkowska-Zbik, D.; Grabowski, R. Direct hydrogenation of CO<sub>2</sub> to dimethyl ether (DME) over hybrid catalysts containing CuO/ZrO<sub>2</sub> as a metallic function and heteropolyacids as an acidic function. *React. Kinet. Mech. Catal.* **2020**, *130*, 179–194. [\[CrossRef\]](#)
135. Wang, P.; Zha, F.; Yao, L.; Chang, Y. Synthesis of light olefins from CO<sub>2</sub> hydrogenation over (CuO-ZnO)-kaolin/SAPO-34 molecular sieves. *Appl. Clay Sci.* **2018**, *163*, 249–256. [\[CrossRef\]](#)

136. Allahyari, S.; Haghighi, M.; Ebadi, A.; Hosseinzadeh, S. Ultrasound assisted co-precipitation of nanostructured CuO-ZnO-Al<sub>2</sub>O<sub>3</sub> over HZSM-5: Effect of precursor and irradiation power on nanocatalyst properties and catalytic performance for direct syngas to DME. *Ultrason. Sonochem.* **2014**, *21*, 663–673. [\[CrossRef\]](#)
137. Miller, J.B.; Rankin, S.E.; Ko, E.I. Strategies in controlling the homogeneity of zirconia-silica aerogels: Effect of preparation on textural and catalytic properties. *J. Catal.* **1994**, *148*, 673. [\[CrossRef\]](#)
138. Román-Leshkov, Y.; Moliner, M.; Davis, M.E. Impact of controlling the site distribution of Al atoms on catalytic properties in ferrierite-type zeolites. *J. Phys. Chem. C* **2011**, *115*, 1096–1102. [\[CrossRef\]](#)
139. Catizzzone, E.; Aloise, A.; Migliori, M.; Giordano, G. The effect of FER zeolite acid sites in methanol to dimethyl ether catalytic dehydration. *J. Energy Chem.* **2017**, *26*, 406–415. [\[CrossRef\]](#)
140. Bonura, G.; Cannilla, C.; Frusteri, L.; Catizzzone, E.; Todaro, S.; Migliori, M.; Giordano, G.; Frusteri, F. Interaction effects between CuO-ZnO-ZrO<sub>2</sub> methanol phase and zeolite surface affecting stability of hybrid systems during one-step CO<sub>2</sub> hydrogenation to DME. *Catal. Today* **2020**, *345*, 175–182. [\[CrossRef\]](#)
141. Bonura, G.; Migliori, M.; Frusteri, L.; Cannilla, C.; Catizzzone, E.; Giordano, G.; Frusteri, F. Acidity control of zeolite functionality on activity and stability of hybrid catalysts during DME production via CO<sub>2</sub> hydrogenation. *J. CO<sub>2</sub> Util.* **2018**, *24*, 398–406. [\[CrossRef\]](#)
142. Ordonsky, V.V.; Cai, M.; Sushkevich, V.; Moldovan, S.; Ersen, O.; Lancelot, C.; Valtchev, V.; Khodakov, A.Y. The role of external acid sites of ZSM-5 in deactivation of hybrid CuZnAl/ZSM-5 catalyst for direct dimethyl ether synthesis from syngas. *Appl. Catal. A Gen.* **2014**, *486*, 266–275. [\[CrossRef\]](#)
143. Sánchez-Contador, M.; Ateka, A.; Aguayo, A.T.; Bilbao, J. Direct synthesis of dimethyl ether from CO and CO<sub>2</sub> over a core-shell structured CuO-ZnO-ZrO<sub>2</sub>@SAPO-11 catalyst. *Fuel Process. Technol.* **2018**, *179*, 258–268. [\[CrossRef\]](#)
144. Ateka, A.; Sánchez-Contador, M.; Portillo, A.; Bilbao, J.; Aguayo, A.T. Kinetic modeling of CO<sub>2</sub>+CO hydrogenation to DME over a CuO-ZnO-ZrO<sub>2</sub>@SAPO-11 core-shell catalyst. *Fuel Process. Technol.* **2020**, *206*, 106434. [\[CrossRef\]](#)
145. Li, X.; Zhang, L.; Zhang, C.; Zhao, M.; Gong, M.; Chen, Y. Effects of La<sub>2</sub>O<sub>3</sub> contents on the Pd/Ce 0.8Zr 0.2O<sub>2</sub>-La<sub>2</sub>O<sub>3</sub> catalysts for methanol decomposition. *J. Rare Earths* **2011**, *29*, 544–549. [\[CrossRef\]](#)
146. Guo, X.; Mao, D.; Lu, G.; Wang, S.; Wu, G. The influence of La doping on the catalytic behavior of Cu/ZrO<sub>2</sub> for methanol synthesis from CO<sub>2</sub> hydrogenation. *J. Mol. Catal. A Chem.* **2011**, *345*, 60–68. [\[CrossRef\]](#)
147. Wang, H.; Wang, Y.; Gao, W.; Guo, W.; Jia, M. Dimethyl ether synthesis from CO<sub>2</sub> hydrogenation on La-modified CuO-ZnO-Al<sub>2</sub>O<sub>3</sub>/HZSM-5 bifunctional catalysts. *J. Rare Earths* **2013**, *31*, 470–476.
148. Yan, N.; Philippot, K. Transformation of CO<sub>2</sub> by using nanoscale metal catalysts: Cases studies on the formation of formic acid and dimethylether. *Curr. Opin. Chem. Eng.* **2018**, *20*, 86–92. [\[CrossRef\]](#)
149. Qin, Z.Z.; Zhou, X.H.; Su, T.M.; Jiang, Y.X.; Ji, H.B. Hydrogenation of CO<sub>2</sub> to dimethyl ether on La-, Ce-modified Cu-Fe/HZSM-5 catalysts. *Catal. Commun.* **2016**, *75*, 78–82. [\[CrossRef\]](#)
150. Zhang, M.H.; Liu, Z.M.; Lin, G.D.; Zhang, H. Bin Pd/CNT-promoted CuZrO<sub>2</sub>/HZSM-5 hybrid catalysts for direct synthesis of DME from CO<sub>2</sub>/H<sub>2</sub>. *Appl. Catal. A Gen.* **2013**, *451*, 28–35. [\[CrossRef\]](#)
151. Chu, R.; Song, C.; Hou, W.; Meng, X.; Miao, Z.; Li, X.; Wu, G.; Wan, Y.; Bai, L. Improved stability of Pd/HZSM-5 bifunctional catalysts by the addition of promoters (CeO<sub>2</sub>, CaO) for the one-step synthesis of dimethyl ether from sulfur containing CO<sub>2</sub> hydrogenation. *J. Taiwan Inst. Chem. Eng.* **2017**, *80*, 1041–1047. [\[CrossRef\]](#)

**Publisher’s Note:** MDPI stays neutral with regard to jurisdictional claims in published maps and institutional affiliations.



© 2020 by the authors. Licensee MDPI, Basel, Switzerland. This article is an open access article distributed under the terms and conditions of the Creative Commons Attribution (CC BY) license (<http://creativecommons.org/licenses/by/4.0/>).